

ReSolve

The next level of simulation



Ultra-fast
aerodynamic boat

PAGE 6

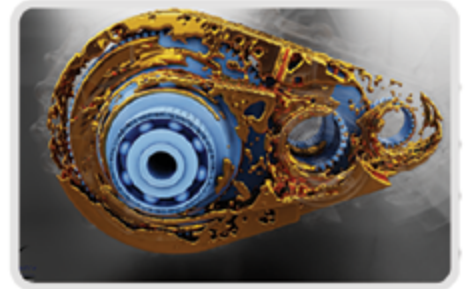
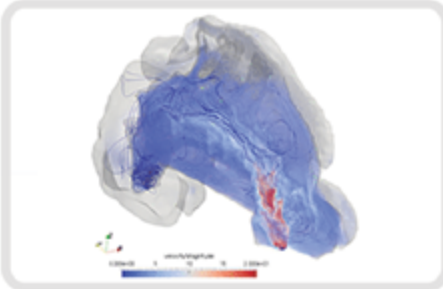
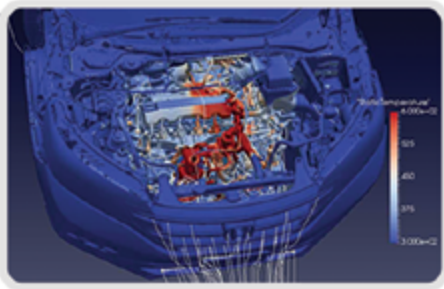
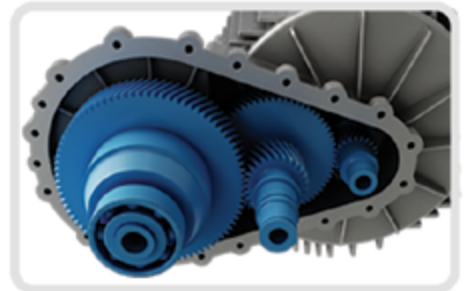
Fully-coupled
CFD engine simulations

PAGE 10

CREMHyg analyzes
transient flow in a multi-piston pump

PAGE 22

OMNIS



Simulating real world phenomena requires
reliable, high-fidelity solutions

NUMECA offers solutions tailored to your application, from cutting-edge meshing technology to Navier Stokes and Lattice Boltzmann solver technology, in a highly advanced environment.

www.numeca.com/products/omnis



Challenges and roads to high-fidelity analysis and design

Industrial CFD is seeing a major (r)evolution due to many converging factors arising from the drive of industry towards high-fidelity modeling, closer to the real behavior of their products. Many elements have to be taken into consideration, in particular, the diversity of flow configurations and applications; the complexity of geometries and physics, the requirements for multidisciplinary analysis and optimization including conjugate heat transfer (CHT) coupling flow and heat transfer: fluid-structure interactions (FSI); fluid-chemistry and multiphase interactions, as in combustion; aero-acoustics coupling flow and noise.

Moreover, designing a component for multidisciplinary interactions is only part of the picture, as proper manufacturing has to be ensured, either through traditional methods or through additive manufacturing. In a more global vision, the integration of the component into the larger environment of its complete transport system or operational plant, leads to further requirements on its interactions with the operational behavior of the complete system, including lifetime assessment and long-term sustainability. Hence, the whole chain of production and life cycle has to be considered in the early design and analysis process.

To address these challenges, NUMECA is continuously extending the functionalities of its existing products as well as preparing exciting new ones. The new environment OMNIS™, developed as a general CAE framework for interacting physics, from CAD to meshing to co-processing and with its openness to external software systems, is a major step offered to industry to enable user-friendly analysis and design.

The central element of a high-fidelity simulation and design environment is tied to the potential of providing performance based, cost and lifetime optimization in a user-friendly and cost-saving approach. However high-fidelity objectives require considering the numerous uncertainties under which the system and the analysis software operate. NUMECA has been leading the European efforts towards methodologies for uncertainty quantification and robust optimization in recent years, which has become a central element of our approach to reliable design. Moving from a deterministic optimization towards a robust optimization whereby the uncertainties are taken into account, for the same global performance objectives and constraints, shows different optimized geometries, the latter ensuring significant enhanced long-term performance.

Along the road towards integrated analysis and design, a long-term objective of the gas turbine industry is the ability to perform full engine simulations, within a single software environment, whereby boundary conditions are imposed only at inlet of the compressor and exit of the power turbine, including unsteady rotor-stator interactions within the compressor and turbine and the ability to model the hot spots effects from the combustor on the turbine inlet guide vanes. The innovative achievements of NUMECA in this direction are representative of the creativity and visions at all levels within our company.

Prof. Charles Hirsch
President, NUMECA International

“ NUMECA is continuously extending the functionalities of its existing products as well as preparing exciting new ones.”

In this issue

Ultra-fast aerodynamic boat

A2V studies the aerodynamics of new fast and fuel efficient passenger transport vessels.

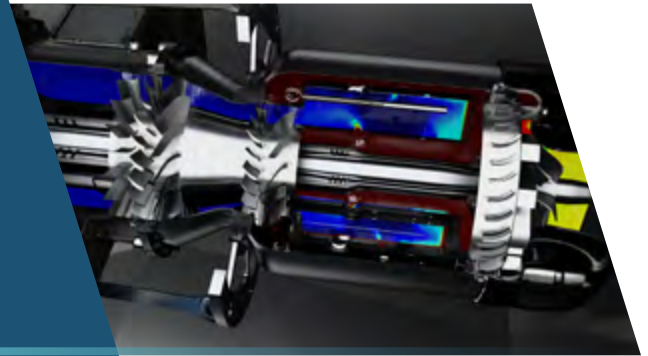
PAGE 6



Fully-coupled CFD engine simulations

Full 3D simulation of a micro gas turbine engine.

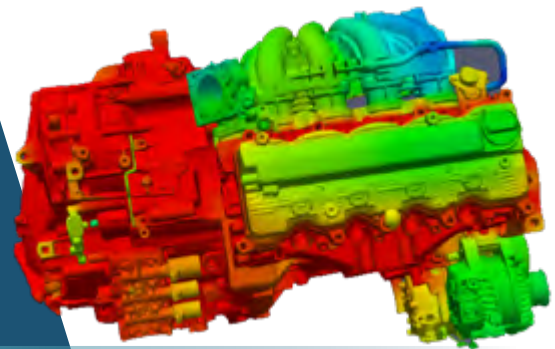
PAGE 10



Honda CR-V: Thermal underhood and underbody simulation

Fully coupled 3D-CFD CHT simulation provides more realistic results in aerodynamic performance and thermal management prediction.

PAGE 18



CREMHyG analyzes transient flow in a multi-piston pump

CremHyG studies flow performance through an axial multi-piston pump to improve the design and obtain better performance.

PAGE 22





OMNIS™:

NUMECA's new generation of CAE design and optimization environment

One common innovative environment to design, analyze and optimize.

PAGE 28



Design optimization of a multi-stage centrifugal compressor

Entechmach optimizes the design of a compressor to improve its performance using FINE™/Design3D.

PAGE 32



NUMECA contributes to the JAXA workshop: a NASA CRM configuration

Aerodynamic prediction at cruise state and high angle of attack.

PAGE 38



Accurate and reliable prediction of the unsteady flow in a radial turbine

Developing a workflow for accurate, reliable and affordable prediction of forced response vibrations in radial turbines, taking into account mistuning effects.

PAGE 44

Would you like to be featured in next issues? Contact us: info@numeca.com

Ultra-fast aerodynamic boat

By **Lionel Huetz**, CEO,
Advanced Aerodynamic Vessels,
France.



Advanced Aerodynamic Vessels (A2V) develops and commercializes a new generation of fast transportation vessels, using aerodynamics to improve energy efficiency. Its revolutionary shape transfers the weight of the ship from the water to the air. As the required propulsive power depends mostly on the weight carried through water, reducing this weight significantly reduces fuel consumption.

Conventional fast vessels

Today's conventional fast vessels' speed depends purely on power. As a consequence increasing speed inevitably comes at the cost of much higher fuel consumption. From an economic and environmental point of view, this leads to an unsustainable cost per passenger.



Meanwhile in a conventional monohull or multihull, fuel consumption per passenger is directly linked to the size of the vessel: the bigger the vessel, the lower the fuel consumption is per passenger when the boat is fully loaded.

“A2V technology has changed the rules by developing and commercializing a new generation of fast and fuel efficient passenger transport vessels. They have designed and patented a wing-like catamaran geometry, which at speed provides aerodynamic lift above the water, alleviating the vessel and thus reducing its power requirements.”

Thanks to the aerodynamic lift, faster means lighter and more efficient

A2V technology has changed the rules by developing and commercializing a new generation of fast and fuel efficient passenger transport vessels. The company markets workboats for the offshore industry, the commercial passenger maritime transport industry, and the states for their patrol, surveillance and rescue missions.

How? They have designed and patented a wing-like catamaran geometry, which at speed provides aerodynamic lift above the water, alleviating the vessel and thus reducing its power requirements. Thanks to the aerodynamic support, above a critical speed, the faster A2V vessels go, the less fuel they use.

“The A2V vessel has a fuel consumption of about 9 litres per passenger per 100km at 50 knots, independent on vessel size, from 10 to 100 passengers, from 12 to 30 meters. As a comparison, present state-of-the-art crewboats typically burn more than 30 litres per passenger per 100km and travel below 40 knots”.

(source: <http://www.aavessels.com/concept/>).

Numerical challenges

One of the challenges in the design of such a vessel is the modelization of the free surface deformation at high speed, to which the stepped hulls are very sensitive since the aft part of the hull is operating in the wake of the forebody. The aerodynamic with the ground effect, both in steady and unsteady conditions, has also been a challenge. In order to model the behavior in the waves with reasonable computational times, A2V carried out systematic aerodynamic analyses and used the results to build a mathematical model. This aerodynamic model was implemented in the hydrodynamic computations using FINE™/Marine dynamic libraries.



“With NUMECA’s software FINE™/Marine, A2V relied entirely on simulation during the design of the fully instrumented 10.5m prototype.”



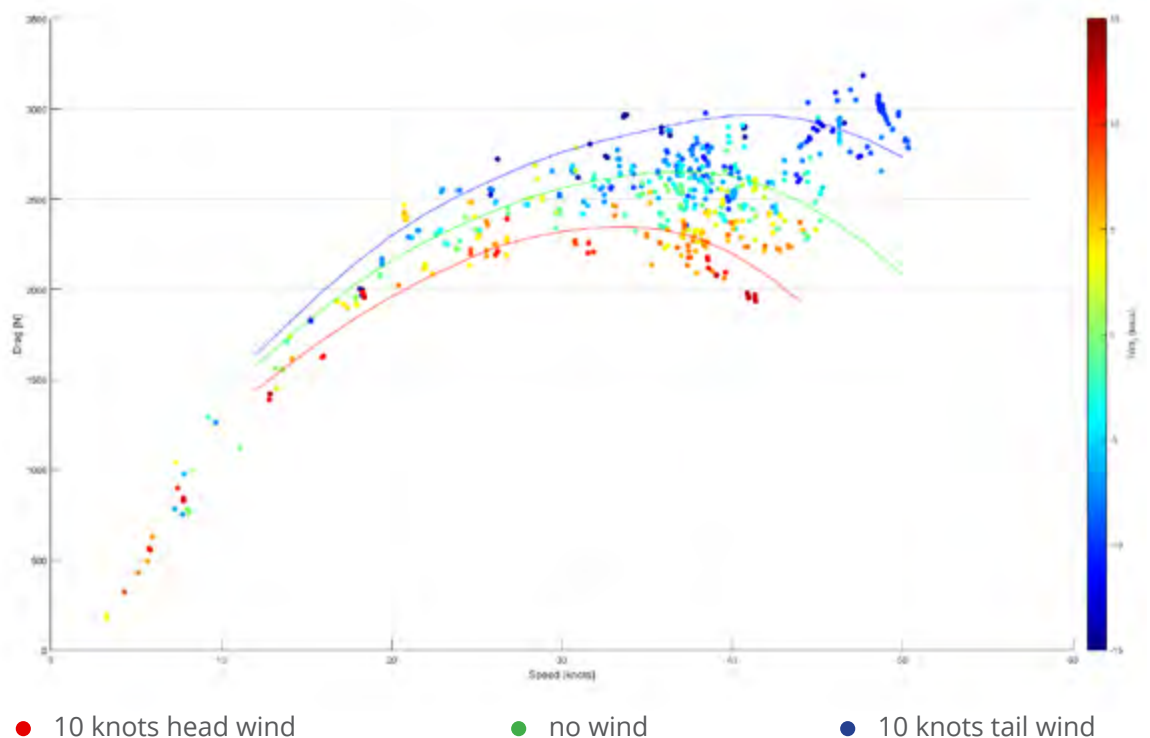
Accurate predictions

Computational Fluids Dynamics is the core of the design approach of this vessel. With NUMECA's software FINE™/Marine, A2V relied entirely on simulation during the design of the fully instrumented 10.5m prototype. The full scale measurements showed that numerical predictions were accurate, as shown in the Figure 1 where numerical predictions are continuous

lines and measurements are dots. The total drag is plotted versus speed for three different cases : (1) 10 knots head wind in red, (2) no wind in green and (3) 10 knots tail wind in blue.

FINE™/Marine also allowed detailed analysis of the flow to refine the design.

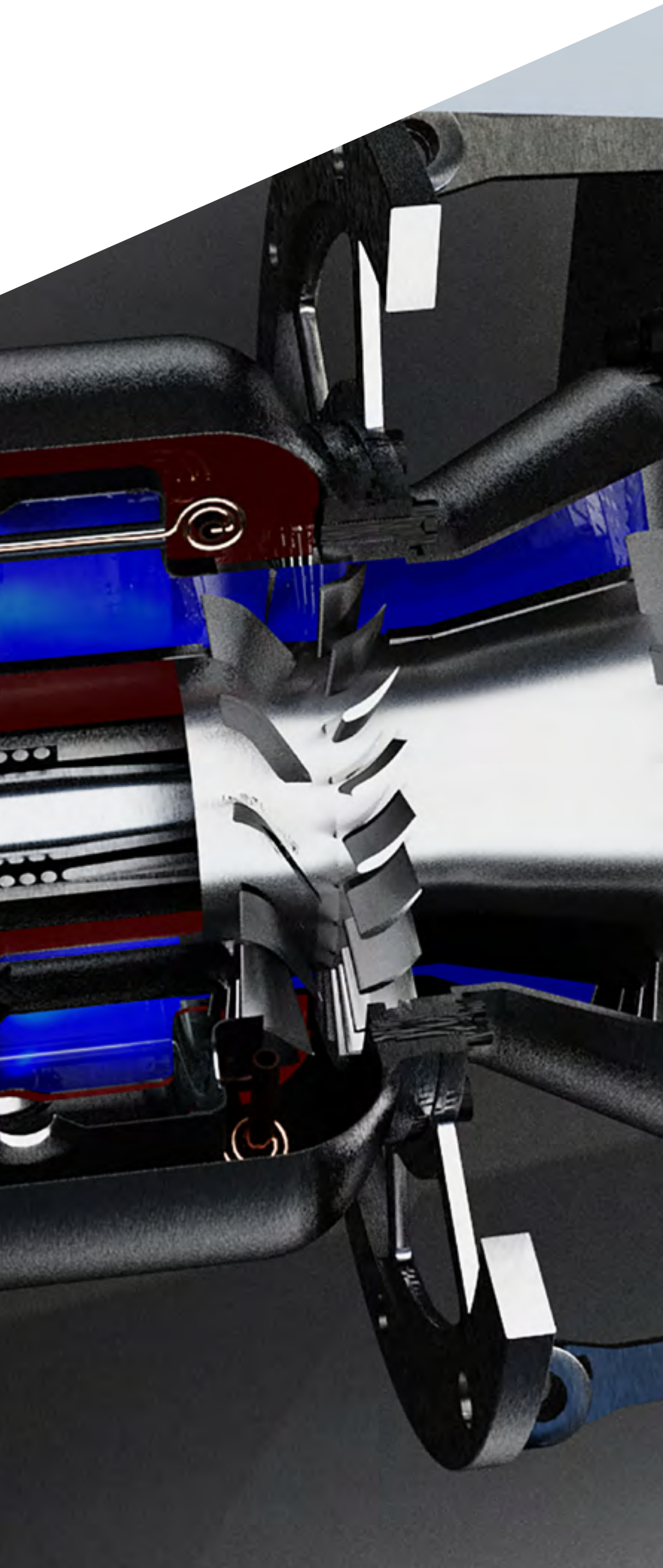
FIGURE 1: Total drag of the A2V prototype in function of the speed: comparison between measurements and CFD predictions.



Fully-coupled CFD engine simulations

By **Mateus Teixeira**,
*Turbomachinery, Preliminary Design
Products & Applications Engineer,
NUMECA International.*

“Improved analysis in the design phase, can add several percentage points to engine efficiency and reduce development cost and time.”



The aerospace industry, like many other industries, is under pressure to drastically reduce its environmental footprint. The Flightpath 2050 goals of the European Union state that by the year 2050 all CO² emissions per passenger kilometer must be reduced by 75%, NO_x by 90% and noise pollution by 65% (relative to the year 2000). [1] One of the ways to achieve these environmental goals is by increasing turbomachinery performance. Improved analysis in the design phase, more specifically development of more reliable predictions, advancement in accuracy, inter-disciplinary and speed of simulation tools, can add several percentage points to engine efficiency and reduce development cost and time. [2][3]

Complexity

One of the main challenges in designing an engine is the complexity in terms of geometrical details (combustion chamber features, turbine cooling holes...) and of interaction effects between the components which must be modelled with accuracy and acceptable computation time.

Full engine simulation methodology

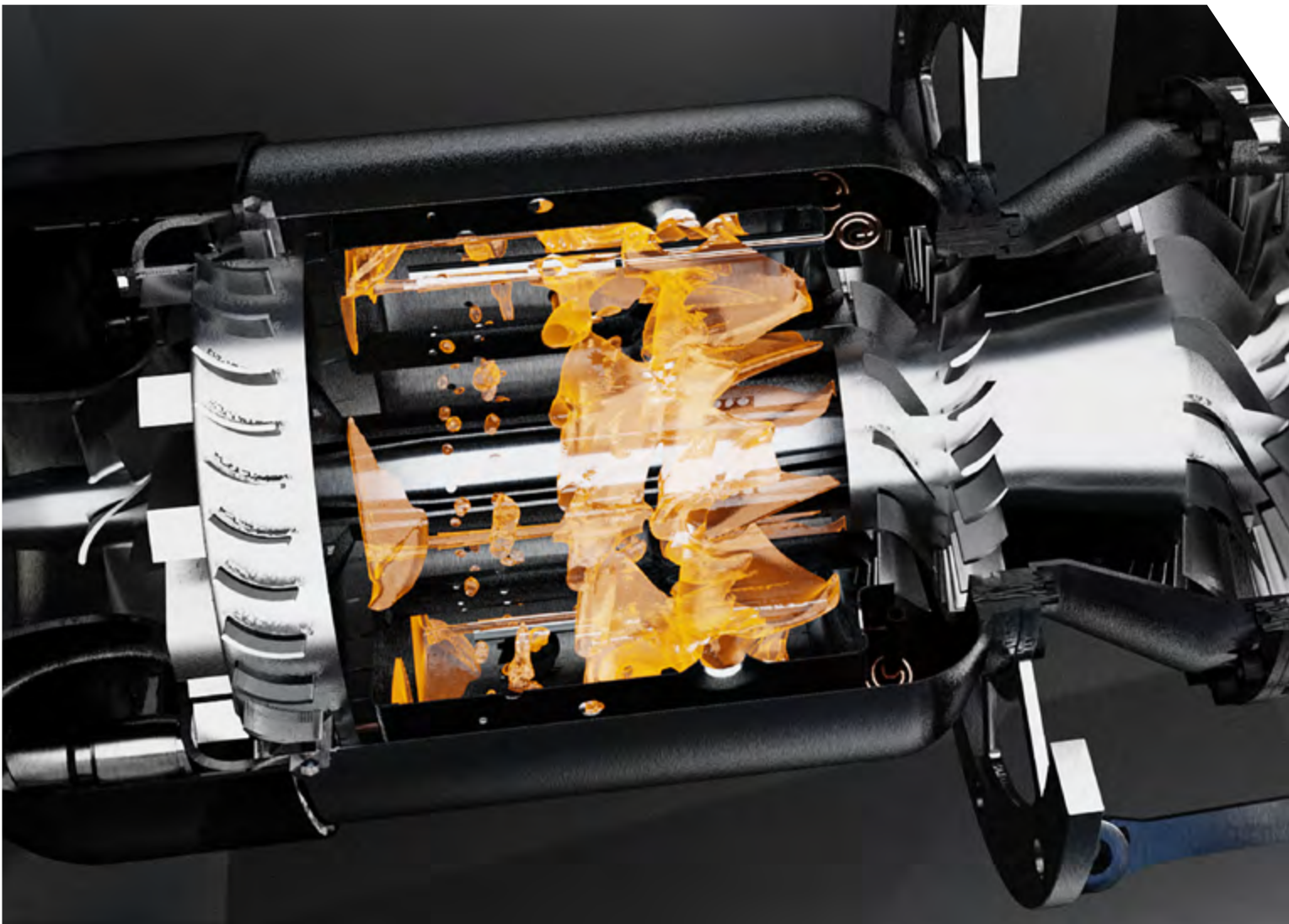
Traditionally engine design in industry has relied on tools like experimental investigation using test or flow bench set-ups, analytical models, empirical/historical data, 1D/2D codes and recently, high fidelity 3D computational fluid dynamics (CFD) for steady and unsteady flow physics modelling. Currently most of the literature work [4-6] and projects conducted at an industrial scale employ a component-by-component analysis approach, where each engine component is studied separately.

Such an approach usually requires assumptions for inlet and outlet boundary conditions for each component and involves a considerable effort in coupling different component analysis tools (often with different modelling degrees of accuracy), leading to a process which is potentially error-prone from the simulation setup point of view and often resulting in significant mismatches between numerical and experimental data.

A one-way coupling approach represents one step further in increasing the accuracy of such simulations. It can be achieved, for example, by extracting outlet profiles of the flow variables from individual converged component simulations and applying them as inlet boundary condition profiles to downstream component runs. Nevertheless, the inter-component interaction is still one-way and the simulation process and results can suffer from similar drawbacks as in the totally uncoupled workflow.

In the two-way coupling methodology all the components are coupled and solved simultaneously in one single simulation. This approach greatly simplifies and accelerates the simulation workflow. Since all the components are considered simultaneously, there is no need to prescribe boundary conditions between the various elements of the aero-engine. This avoids running simulations where the states at the interface between the different components have to be guessed.

FIGURE 1 : Three types of full engine simulation methodologies



The full engine CFD numerical modeling methodology can be mainly categorized in three levels:

- [1] **Steady-state RANS simulations:** computationally low cost and usually involving a single meshed blade passage per turbomachinery row with mixing-plane interfaces between components;
- [2] **Unsteady-state RANS time domain simulations:** computationally expensive, employing several meshed blade passages per turbomachinery row, usually requiring many time steps to reach periodic flow conditions and providing solutions for a single clocking configuration per run;
- [3] **Unsteady-state RANS frequency domain simulations:** 2-3 orders of magnitude faster than time domain method computations, employing a single meshed blade passage per turbomachinery row, providing improved rotor-stator interfaces modeling and allowing arbitrarily clocked solution reconstruction in time.

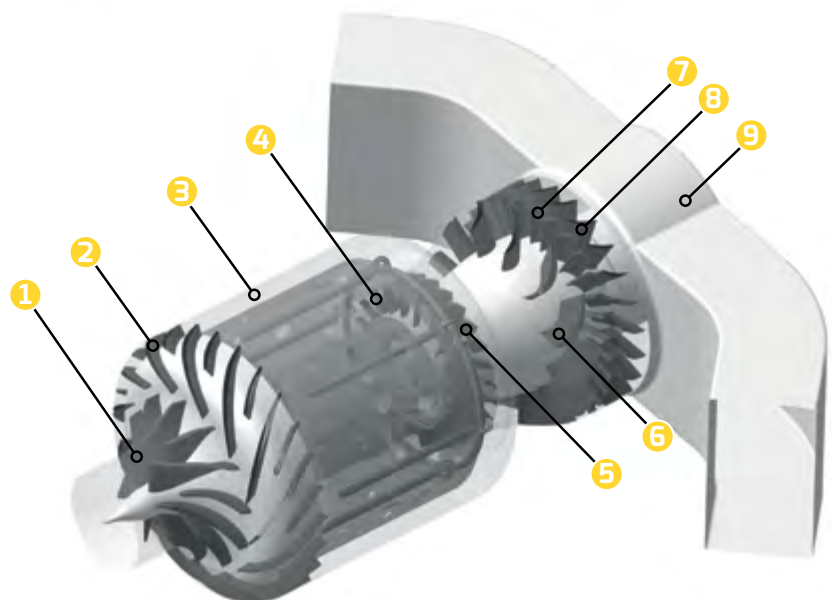
NUMECA's approach to full engine CFD simulation

A full 3D aerodynamic simulation of a complete gas turbine engine, applied to a micro turbine case has been conducted at NUMECA. The analysis was comprised of a single fully-coupled 3D CFD simulation for the flow of a KJ66 engine redesign. The injection and burning of fuel inside the combustion chamber are modeled with a simplified flamelet model. Using advanced RANS treatment with inputs from Nonlinear Harmonic (NLH) method (available as module for FINE™/ Turbo), tangential non-uniformities are captured and the flow physics of the interaction between compressor, combustor and turbine are assessed.

Case description

The selected test case is a redesign version of the KJ66 micro gas turbine (Figure 2). The Figure 2 shows the layout of the redesigned version of the KJ66 micro gas turbine used in the full engine computation. The centrifugal compressor is mounted at the engine entrance and it is composed of an impeller and a bladed diffuser row. The combustion chamber is followed by a high-pressure turbine (HPT), which drives the compressor, and a low pressure turbine (LPT), which would drive a propeller in an independent shaft. An exhaust hood is connected to the last LPT row at the engine exit.

FIGURE 2 : Layout of the KJ66 micro gas turbine



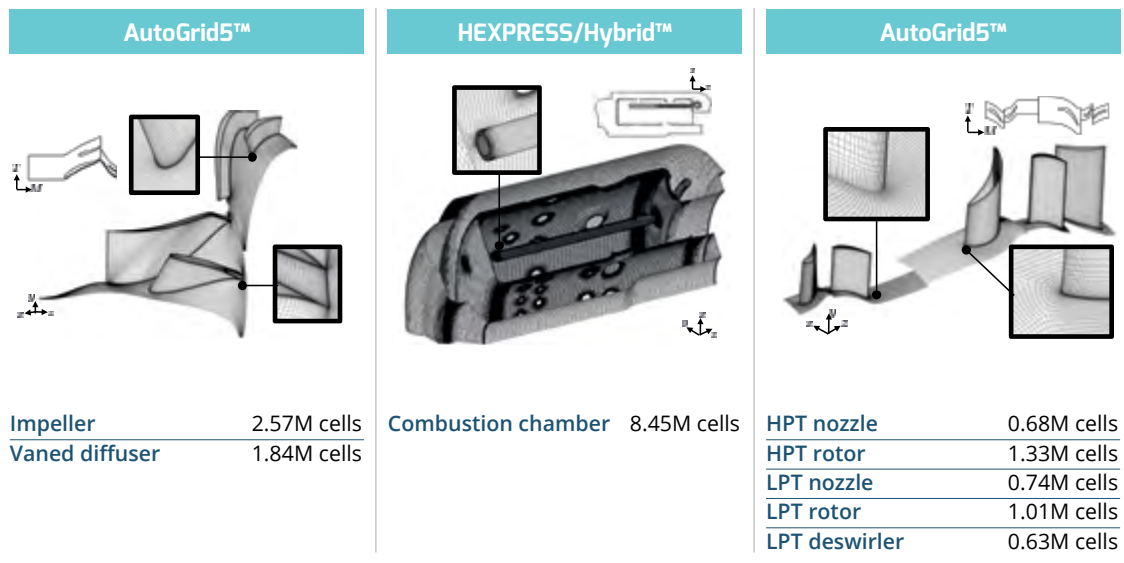
- | | | |
|----------------------|--------------|------------------|
| 1 Impeller | 4 HPT nozzle | 7 LPT rotor |
| 2 Vaned Diffuser | 5 HPT rotor | 8 LPT deswirler |
| 3 Combustion chamber | 6 LPT nozzle | 9 Exhaust system |

Simulation setup

The computational domain encompassed one blade passage for each turbomachinery blade row, a 60° sector for the combustion chamber (containing one fuel injector) and half exhaust hood. The three-dimensional mesh for the blade rows (compressor and turbine rows) was generated automatically using Autogrid5™, NUMECA's turbomachinery dedicated full automatic hexahedral

block-structured grid generator. The mesh for the combustion chamber and exhaust hood was generated with HEXPRESS/Hybrid™, NUMECA's unstructured hex-dominant conformal body-fitted mesher for arbitrary complex geometries. The entire mesh has 19.20 million points.

FIGURE 3 : Compressor, combustion chamber and turbine 3D mesh view and blade-to-blade layout (shrouds are omitted).



As a first investigation, the steady RANS computation is performed with the Spalart-Allmaras turbulence model. Ambient total quantities are imposed at the engine inlet ($p_0 = 101325$ Pa and $T_{01} = 293$ K) with specified axial velocity direction and static pressure is fixed at the outlet. The fuel injection is specified with static temperature ($T_f = 300$ K) and axial velocity of -120 m/s. Solid walls are assumed smooth and adiabatic.

The convergence history is checked by following the evolution of the mass flow, the pressure ratio, and net torque between the HPT rotor and the impeller ($Mz = Mz^{HPT} - Mz^{comp}$). The computation is launched in parallel on 144 processors on a computing cluster. In a second step, the computation is restarted with an improved rotor-stator connection based on the NLH method.

Combustion model

The injection and burning of fuel inside the combustion chamber are modeled with a simplified flamelet model implemented in OpenLabs™. With this model, an additional equation is solved for the mixture fraction f , with the flame temperature as function of the composition.

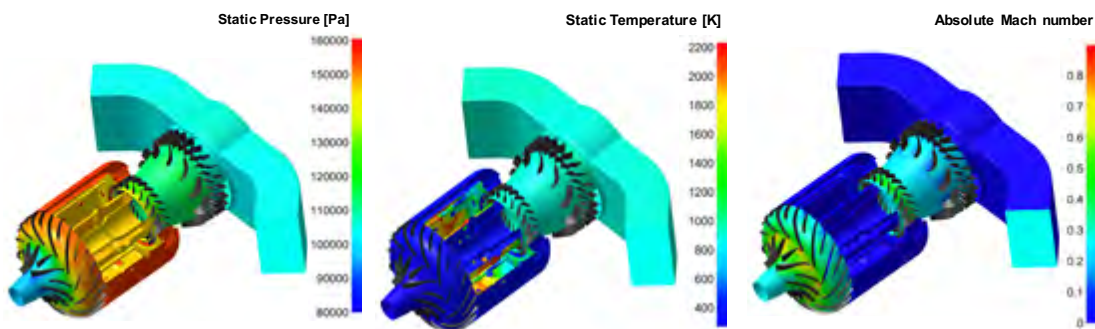
Results

Steady-state computation

The convergence history of mass flow rate error between the engine inlet and outlet drops to less than 0.2% after 25000 iterations in approximately 24 hours of wall clock time. The net torque Mz reaches a final value of +0.21 N.m when the couple impeller-HPT rotor spins at -80000 rpm, meaning that the turbine produces enough torque to drive the compressor and both components are very close to be load balanced.

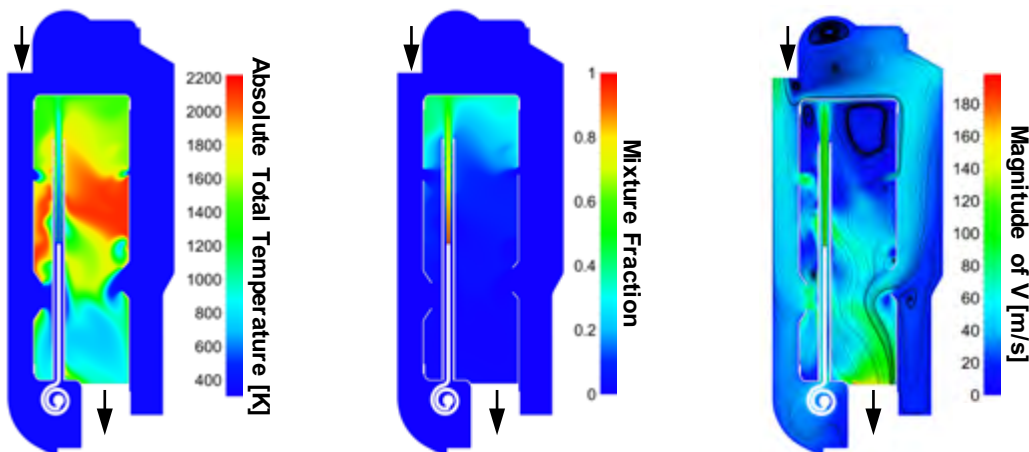
The Figure 4 shows the static pressure, static temperature and absolute Mach number distributions at midspan of the compressor and turbine as well as in the solid walls of the combustion chamber and exhaust hood. The flow fields are continuous across the machine with a gradual raise of Mach number through the impeller and subsequent conversion of the kinetic energy into pressure across the diffuser. At approximately 160 kPa, air reaches the combustion chamber where the simulated combustion process takes place with a relatively small pressure loss. The maximum temperature at the combustion chamber is around 2200K at the combustor inner chamber. The hot gases from the combustion enter the HPT at approximately 983K and are expanded through the downstream blade rows, exiting the machine at 932K.

FIGURE 4 : Static pressure (left), static temperature (center) and absolute Mach number (right) distribution at midspan of the compressor and turbine and at the solid walls of the combustion chamber and exhaust hood.



As shown in the Figures 5, the mixture fraction color contour successfully depicts the fuel stream entering the combustion chamber with $f = 1$ and the combustion gases gradually reaching a value of 0.02 at the component exit. The effect of the holes in the inner chamber walls can be noticed in the magnitude of velocity color contour: they provide a flow of compressed air, acting as oxidizer for the combustion process, to mix with vaporized fuel and achieve ignition.

FIGURE 5 : Absolute total temperature, mixture fraction and magnitude of absolute velocity distribution at the meridional plane of the combustion chamber.



NLH Computation

The results from the RANS computation using a mixing plane treatment at the rotor stator interface can be compared to the results of the NLH analysis. In particular, it is interesting to note the effect of the improved connection approach with respect to the inter-components interactions.

The Figures 6 and 7 show similar results on the mass flux for both simulations at the exit of the combustion chamber.

A pattern linked to the periodicity of the fuel pipes and to the combustion zones can be observed. The transfer of information from the combustor outlet to the adjacent downstream HPT nozzle is different for the RANS simulation and its NLH counterpart. The mixing plane approach shows no tangential non-uniformities, while the NLH rotor-stator treatment proves to be a low cost first step in capturing tangential non-uniformities.

FIGURE 6 : Mass flux at the outlet of the combustion chamber and at the inlet of the HPT for the steady-state (left) and NLH 0 harmonic (right) simulations.

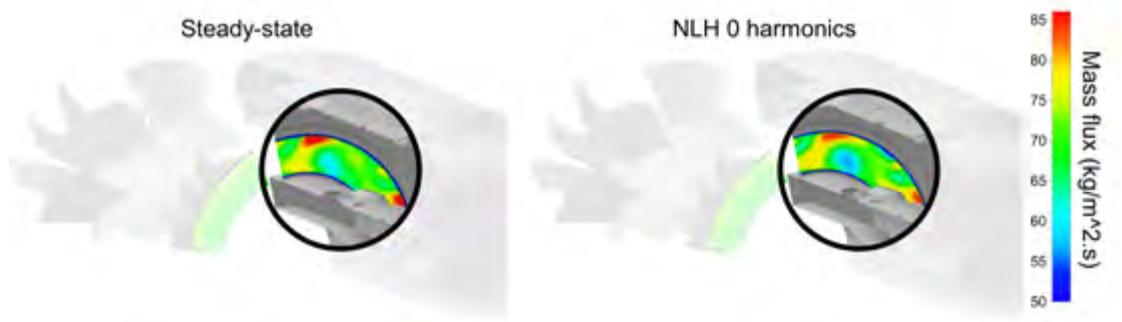


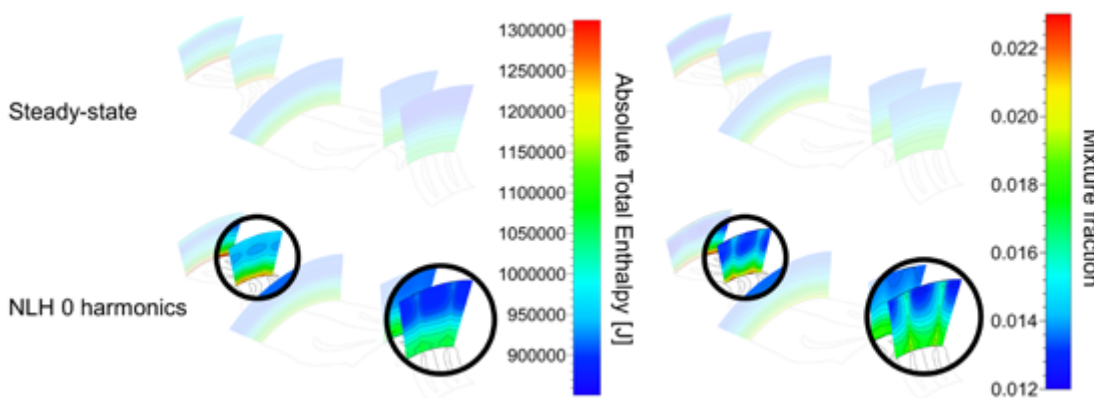
FIGURE 7 : Mass flux at the outlet of the combustion chamber and at the inlet of the HPT for the steady-state (left) and NLH 0 harmonic (right) simulations.



The Figure 8 shows the results for absolute total enthalpy and mixture fraction at the HPT and LPT inlet connections. The azimuthal averaging used in the mixing plane approach, where tangential non-uniformities are not perceived by downstream components, can be

noticed for the RANS simulation. In contrast, the Fourier decomposition together with the local non-reflective boundary treatment used in the NLH method is able to show a slight improvement at the interfaces.

FIGURE 8 : Absolute total enthalpy and mixture fraction at the inlet of the HPT and LPT blade rows for the steady-state (top) and NLH 0 harmonic (bottom) simulations.



Conclusions

A successful simulation of the three-dimensional flow of a complete micro gas turbine engine has been achieved, on the basis of a fully-coupled 3D CFD simulation of a redesigned version of the KJ66 micro gas turbine. Compared to the component-by-component analysis, the fully coupled approach enables the solution

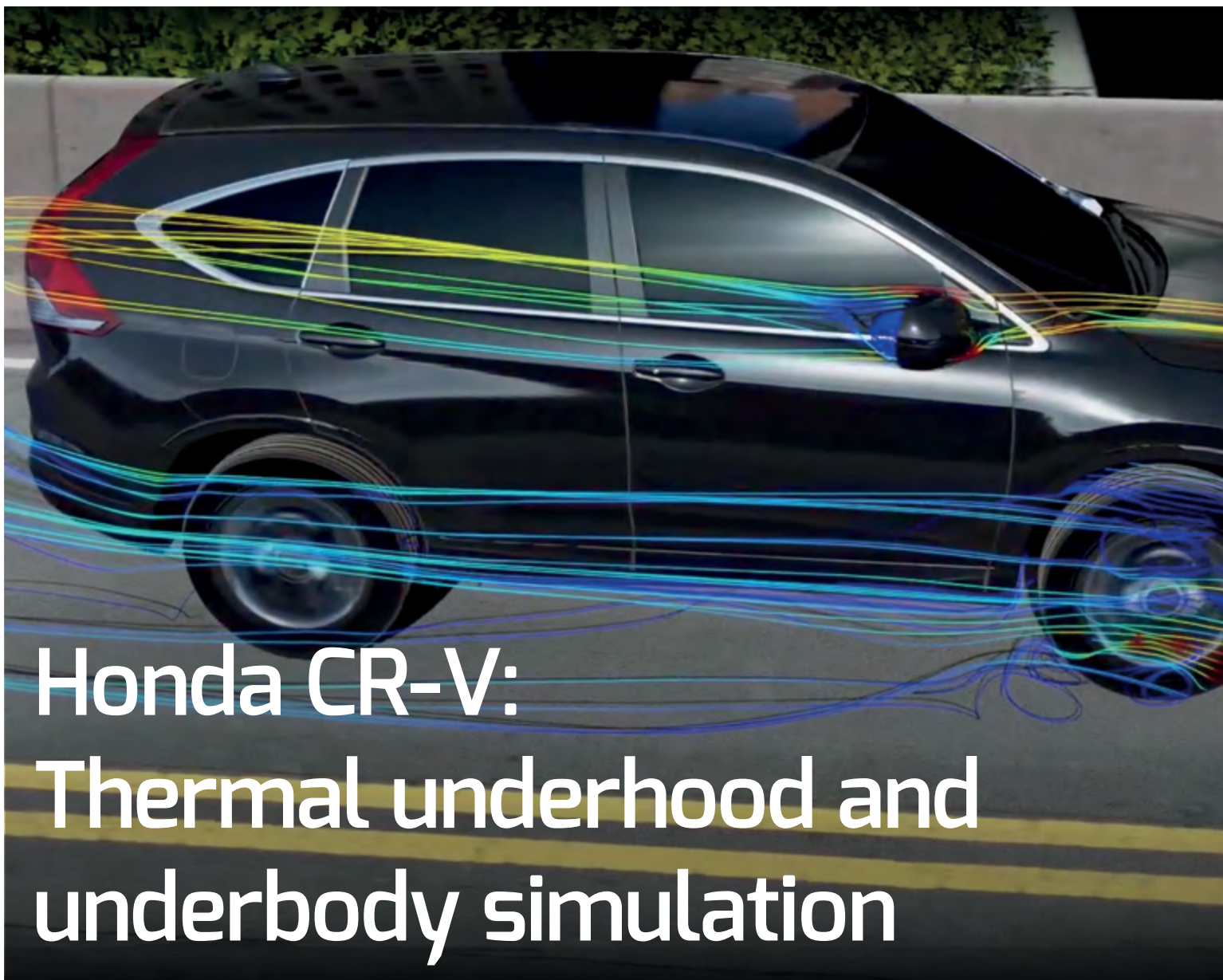
of the whole engine in one single simulation. Furthermore it simplifies the simulation workflow as only the engine inlet and outlet pressures, the rotating speed and the fuel mass flow rate need to be prescribed.

Source: Teixeira M, Romagnosi L, Mezine M, et al. *A Methodology for Fully-Coupled CFD Engine Simulations, Applied to a Micro Gas Turbine Engine*. ASME. *Turbo Expo: Power for Land, Sea, and Air*, Volume 2C: Turbomachinery ():V02CT42A047. doi:10.1115/GT2018-76870.

References

- [1] Flightpath 2050: Europe's Vision for Aviation, 2011, <http://www.acare4europe.org/sria/flightpath-2050-goals>.
- [2] National Academies of Sciences, Engineering, and Medicine, 2016, "Commercial Aircraft Propulsion and Energy Systems Research: Reducing Global Carbon Emissions", Washington, DC: The National Academies Press
- [3] Mavriplis D., Darmofal D., Keyes D., Turner M., 2007, "Petaflops opportunities for the NASA Fundamental Aeronautics Program", 18th AIAA Computational Fluid Dynamics Conf., Miami, FL, AIAA paper 2007-4084.
- [4] Xiang J., Schluter J. U., Duan F., 2016, "Study of KJ-66 Micro Gas Turbine Compressor: Steady and Unsteady Reynolds-Averaged Navier–Stokes Approach", *Proceedings of the Institution of Mechanical Engineers Part G Journal of Aerospace Engineering*.
- [5] Gonzalez C.A., Wong K.C., Armfield S., 2008, "Computational study of a micro-turbine engine combustor using large eddy simulation and Reynolds averaged turbulence models", ANZIAM J. 49 (EMAC2007) pp.C407–C422, C407.
- [6] Turner M., 2000, "Full 3D Analysis of the GE90 Turbofan Primary Flowpath", NASA/CR—2000-209951.

“ Compared to the component-by-component analysis, the fully coupled approach enables the solution of the whole engine in one single simulation.”



Honda CR-V: Thermal underhood and underbody simulation

By **Lohitasyudu Gorli**,
*Aero, Multiphysics &
Combustion Products
& Applications Engineer*
and **Kilian Claramunt**,
*Multiphysics Head of
Group* and **Yingchen
Li**, *Openlabs & Adjoints
Responsible*,
NUMECA International.

With the growing availability and cost-effectiveness of computational resources, computational fluid dynamics (CFD) simulations should be able to smoothly handle complex physics and their interactions. Moreover the development cycles in the automotive industry are constantly getting shorter, which drives the demand for reliable, automated simulation processes providing accurate results within a short time frame.

Against this background, NUMECA presents a comprehensive toolchain for fully coupled simulations, addressing the thermal management of a complete vehicle, drastically reducing overall engineering time by using HEXPRESS™/Hybrid for meshing and FINE™/Open with OpenLABs for the flow and thermal predictions.

FINE™/Open with OpenLabs allows large scale coupled simulations, taking into account the

external flow, rotating components, porous media, conjugate heat transfer, heat exchanger modelling and radiation in one single simulation. The reliability of this fully coupled approach was proven by an industrial case of the Honda CR-V car. Special focus was put on the unstructured conformal multi-block meshing using HEXPRESS™/Hybrid, which represents a crucial starting point.

Project Description

A fully coupled thermal 3D-CFD RANS simulation of a comprehensive and detailed car model for the Honda CR-V SUV model is performed. The simulation mainly focuses on the thermal aspects within the under hood of the car. All relevant sources of heat are taken into account, including the engine, the exhaust system, the radiator and condenser, as well as the fans attached to it.



Meshing

This simulation requires a high quality mesh containing blocks for all parts of the car, which either act as heat sinks or sources or which play a significant role in heat conduction, convection or radiation.

The definition of the adjacent mesh blocks and the corresponding interfaces is done automatically by the unstructured meshing tool HEXPRESS™/Hybrid, which reduces significantly the engineering time required to set up the computation. This also ensures conformal connections between all blocks, thus eliminating inaccuracies typically caused by the interpolation due to non-matching block connections.

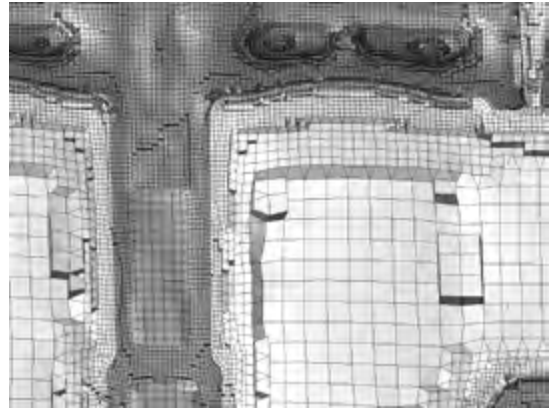
HEXPRESS™/Hybrid directly addresses the demands of the automotive industry. The original, imperfect CAD data can be imported right away with reduced need for CAD pre-processing or manual adaptation of the input geometry again saving a significant amount of engineering time.

FIGURE 1 : Combined view of geometry and mesh of Honda CR-V model



The second kind of applications, called “closed thin wall” method, is used for multi-block/ multi-material meshing. Typical examples are porous blocks inside a fluid, fluid/solid block meshing for conjugate heat transfer problems and rotating parts.

FIGURE 2 : Cut Section of the Engine Block with air inside the exhaust manifold and external air where the mesh is fully conformal



In total, the multi-block mesh contained 57 different blocks, all of which are connected through nodal-conformal interfaces. For the feasibility study, no viscous layers were inserted in the first attempt. Instead, wall functions were used to model the flow in the boundary layer. This approach led to a mesh size of 420 million Cells, covering fluid and solid domains, created in less than 9 hours on 32 cores.

Conjugate heat transfer

In order to obtain realistic and accurate heat transfer predictions, the different solid parts of the geometry are taken into account in the energy equation with the resolution of the heat conduction equation. The thermal properties of the solid bodies are characterized by their conductivity coefficient. At the solid-fluid interface, the heat flux is implicitly applied based on the gradient of the temperature between the solid and fluid bodies.

Surface-to-Surface Radiation

The exchange of radiative energy between the surfaces of the engine, exhaust pipe and other frames is virtually unaffected by the air flow and a surface-to-surface (S2S) radiation model is therefore chosen to simulate the radiative heat exchange between hot and cold components.

It is usual to assume that all surfaces are gray diffuse emitters (and thus, absorbers), as well as gray diffuse reflectors. With these assumptions, the radiosity-irradiosity method [2] can be applied, requiring the calculation of the view factors. In FINE™/Open with OpenLabs™, the Stochastic Ray Tracing method [3,4,5,6] is used to calculate these view factors.

With the high performance of the ray tracing algorithm, the view factor of the Honda car can be computed in one hour, with more than 200 processors, using 1,000 rays shooting per boundary facet.

The coupling of radiation with the flow can be applied to a selectable level. When the radiation is strong, it may need more cycles of the coupling: solving radiosity equations for radiative heat fluxes with current boundary temperature - applying boundary conditions with the computed radiative heat fluxes.

Heat exchanger model

The radiator and condenser are modelled as porous media with isotropic pressure loss. OpenLabs™ is used to customize these two blocks so that the pressure drop across each block matches experimental data.

For the radiator block, in addition to the pressure drop, a coupled strategy between the steady-state CFD calculation and a thermal 1D calculation is defined. The coolant temperature varies throughout its flow path, with a non-uniform heat rejection from the radiator over the block. The heat exchanger subsystem is formed by the CFD mesh for the primary fluid, the air, and an overlapped 2D coarser

mesh along the direction of the auxiliary fluid flow defined by the coolant. This approach of modelling the heat exchanger core by splitting it into macroscopic cells provides more realistic solutions for the heat rejection compared to a uniform heat source term.

Rotating Machinery

FIGURE 3 : Counter-rotating fans in front of radiator and condenser



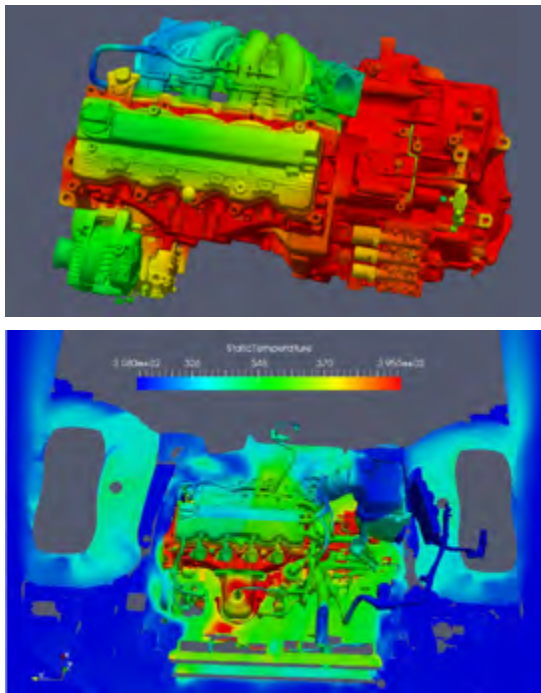
For the counter-rotating fans, two models are available in FINE™/Open with OpenLabs. The added momentum and energy could be introduced using an actuator disk model which doesn't contain the geometry, but only models the effect on the flow. The definition of the source terms would be possible through the programmable interface OpenLabs™. The other method is to build cylindrical blocks containing the fans and connect them to the surrounding domain using a rotor/stator interface. This second approach was chosen in combination with a frozen rotor interface. Although this represents only a snapshot in time, its advantage is the high robustness and low computational cost compared to a pitchwise averaging. The blocks containing the fans are conformally connected to the outer air domain.



Results

The fully coupled CHT simulation provides much more realistic results in both aerodynamic performance and thermal management prediction. Figure 4 gives the external aerodynamic view of the car, showing the pressure distribution and the streamlines around the car. Pressure distribution in front the wheel shows the complexity of the flow under the car, which has a strong effect on the thermal prediction of the underbody. Therefore a fully coupled CHT simulation is adopted here.

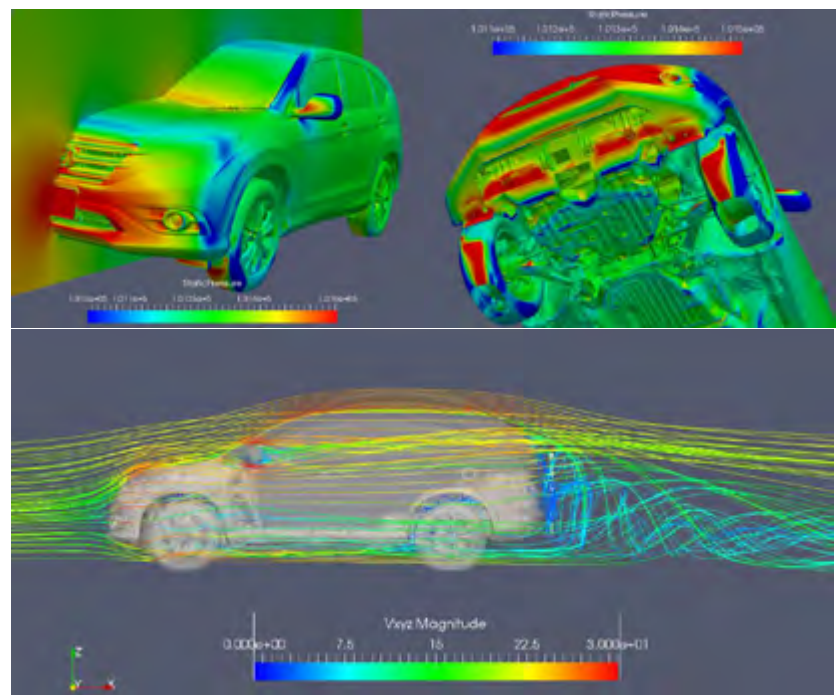
FIGURE 5 : Temperature of engine surface and the horizontal cutting plane around engine



As can be seen in Figures 5, a temperature distribution is visible on both the engine and muffler surfaces, showing that neither the temperature nor the heat flux can be assumed as constant along the surface. The thermal interactions in both the engine compartment and the exhaust system can therefore only be modelled accurately by the use of a coupled CFD simulation which captures the conjugate heat transfer effects.

Source: Posselt F., Gorli L., Claramunt K., Leonard B., Li Y. (2017) Thermal behavior of a SUV car with a fully coupled 3D-CFD CHT simulation. In: Bargende M., Reuss HC., Wiedemann J. (eds) 17. Internationales Stuttgarter Symposium. Proceedings. Springer Vieweg, Wiesbaden. https://doi.org/10.1007/978-3-658-16988-6_38

FIGURE 4 : Static pressure distribution in the front part of the car and external aerodynamics view



Figures 6 and 7 show the temperature distribution on the exhaust pipe and the underbody. The large temperature differences cause a strong radiation heat transfer. Thus, to achieve accurate thermal predictions, the direct coupling of CHT with radiation model has to be adopted.

FIGURE 6 : Temperature of the exhaust pipe

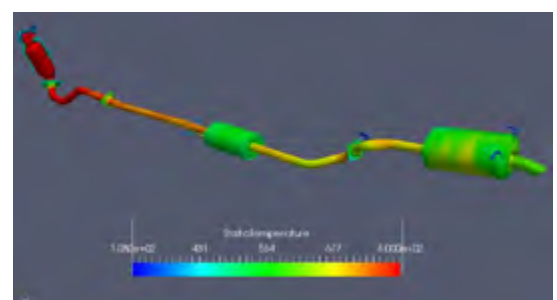
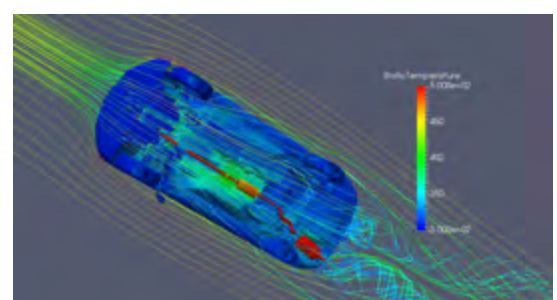


FIGURE 7 : Static Temperature on the exhaust system and flow structure at the underbody



CREMHyG analyzes transient flow in a multi-piston pump



By **Claude Rebattet**,
*Head of CREMHyG laboratory,
University of Grenoble Alpes,
France.*

“CREMHyG decided to use NUMECA’s Lattice Boltzmann solver OMNIS™/LB, as they needed a solution well adapted for complex geometries and complicated displacements.”

The Grenoble Hydraulic Machinery Research and Testing Centre (CREMHyG) is a laboratory of the Grenoble Institute of Technology (Grenoble INP).

The turbomachinery testing platform CREMHyG's main areas of activity focus on hydroelectric energy and associated machines (pumps, turbines and pump-turbines). They test hydraulic applications such as hydropower, hydraulic storage, liquid propulsion, pumping and others.

CREMHyG Lab collaborates with industrial companies to develop the future of hydroelectric energy. The experimental platform is equipped with large facilities of up to 300 kW to perform contractual testing under the International Electrotechnical Commission (IEC) standard of reduced models of pumps, turbines and reversible pump turbines, and with smaller ones of up to 20 kW for research and training. The experiments and tests focus on steady and unsteady flows through rotating machinery: Francis turbines, reversible PSPs, axial inducers, centrifugal or piston pumps and others. Research is targeted to improve stability and security of the functional domain in critical conditions such as cavitation, multiphase flow and off design behaviors.

In order to compare simulation and test, a first demonstrator of a piston pump developed for drilling applications has been scaled $\frac{1}{4}$ to be powered by a 10 kW motor. We present the first investigation on the simulations performed with NUMECA's Lattice Boltzmann solver OMNIS™/LB.

Design of a swashplate axial piston pump

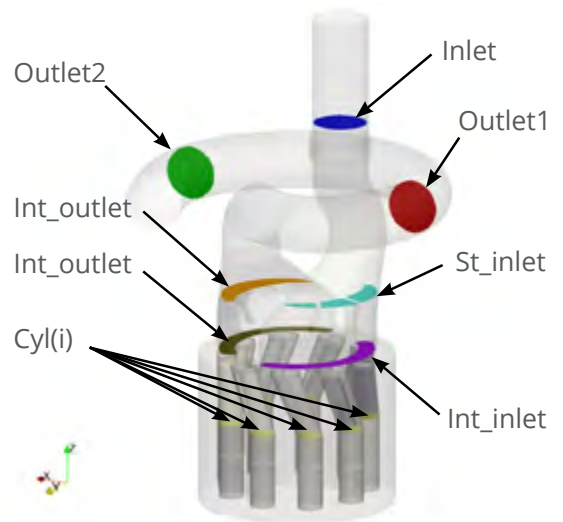
One of the objectives is to design a swashplate axial multi-piston pump without check valves to distribute the flow to pistons. The pump consists of two parts: a stator, composed of two conducts that are communicated with inlet and outlet to distribute the flow, and a rotor, moving 9 pistons in a barrel. The electric and

mechanical design permits the use of variable speeds and inclinations of the plate to optimize flexible discharge and starting and stopping operations without torque overloads or strong pressure peaks. Each piston interacts with the stator, the rotor-stator interface connects through a contact surface between rotating barrel and static valve plate.

Simulation of a swashplate axial piston pump

The main objective of the fluid simulation is to analyze flow circulation and pressure transients in order to prevent mechanical solicitations linked to alternate displacement of pistons and rotor-stator interaction in the interface volume. The following locations have been analyzed: cylinders, interface stator-rotor (stator side), stator, outlet pipe and inlet pipe.

FIGURE 1: Components and meshed parts of the axial piston pump



Benchmark on flow performance analysis

In this benchmark, CREMHyG is seeking to analyze the flow performance through the axial multi-piston pump in order to collect data for design optimization towards better performance. This way the study of the overall behavior of the pump would enable understanding of the design impact on the performance. To do so, CREMHyG has decided to use NUMECA's Lattice Boltzmann solver OMNIS™/LB, as they needed a solution well adapted for complex geometries and complicated displacements.

From a preliminary CAD design of the pump and a simulation model taking into account the displacement of all the pistons (rotation and translation), the CFD model has been used to analyze the unsteady flow through this complex geometry; to identify pressure fluctuations and distribution at different stations; and to estimate global performances concerning torque and power.

To understand the behavior of the piston pump, two different regimes and outlet pressures have been simulated under the same discharge flow rate:

- » **Case 1:** Low outlet pressure and rotational speed, high stroke.
- » **Case 2:** High outlet pressure and rotational speed, low stroke.

And two flow variables have been analyzed:

- » **Relative pressure:** pressure difference between inlet and outlet.
- » **Mass flow rate.**

Results

1. Relative pressure

FIGURE 2 : Relative pressure (Pa)

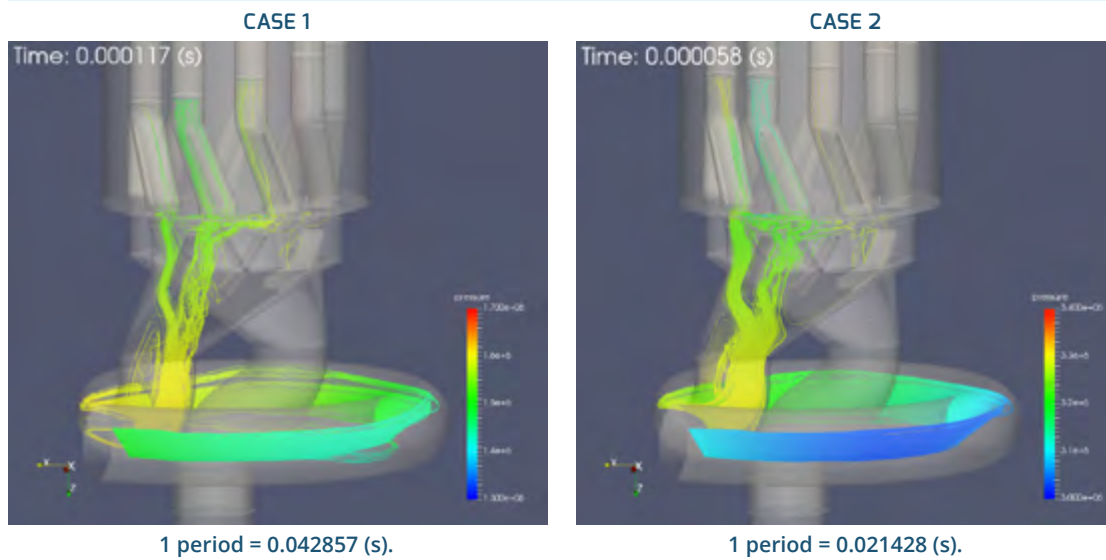
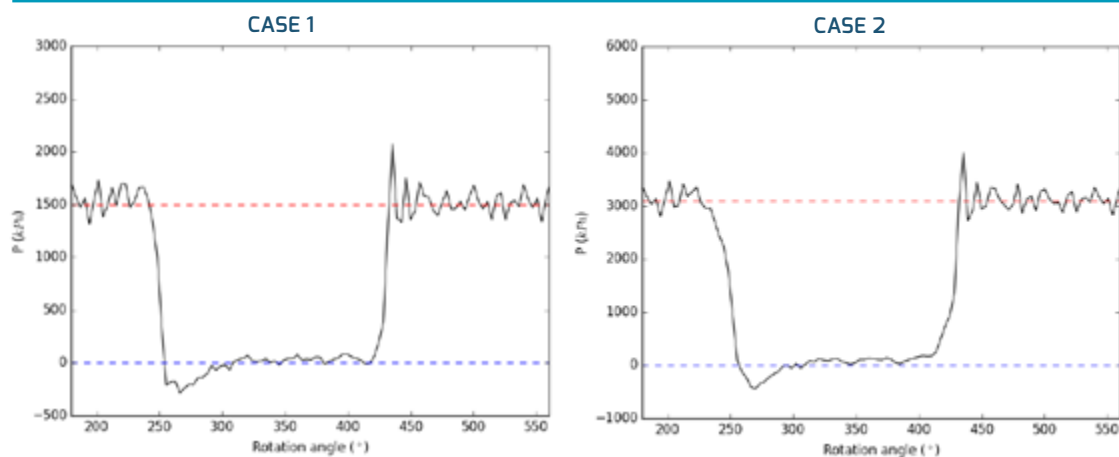


FIGURE 3 : Relative pressure - Cylinder



The pressure cycle seems to be linear as no substantial differences in shape were found between both cases. Risk of cavitation however is larger in Case 2, where the lowest pressure is found at the beginning of the intake stroke. Pressure oscillations are generated at the interface rotor-stator, where regions of liquid at different pressures are put in contact. The main mode of these oscillations corresponds therefore to the product of the rotational speed and the number of pistons. The amplitude also seems to correlate with the pressure difference between inlet and outlet so that linearity holds. These pressure oscillations propagate throughout the whole pump causing unsteady perturbations on the streamlines.

2. Mass flow

FIGURE 4 : Axial velocity (m/s) - Cylinder cut

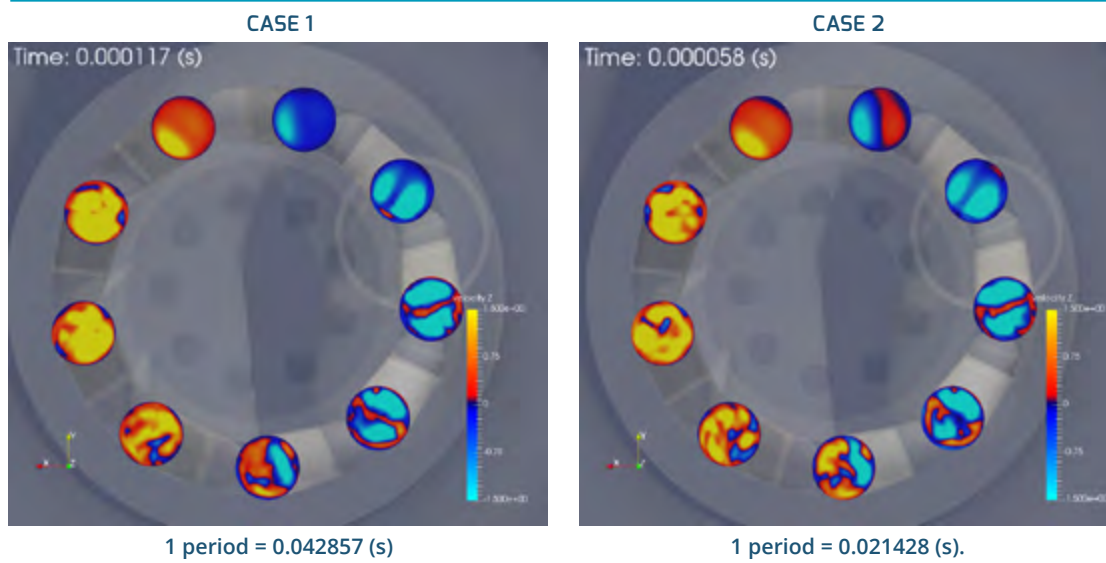
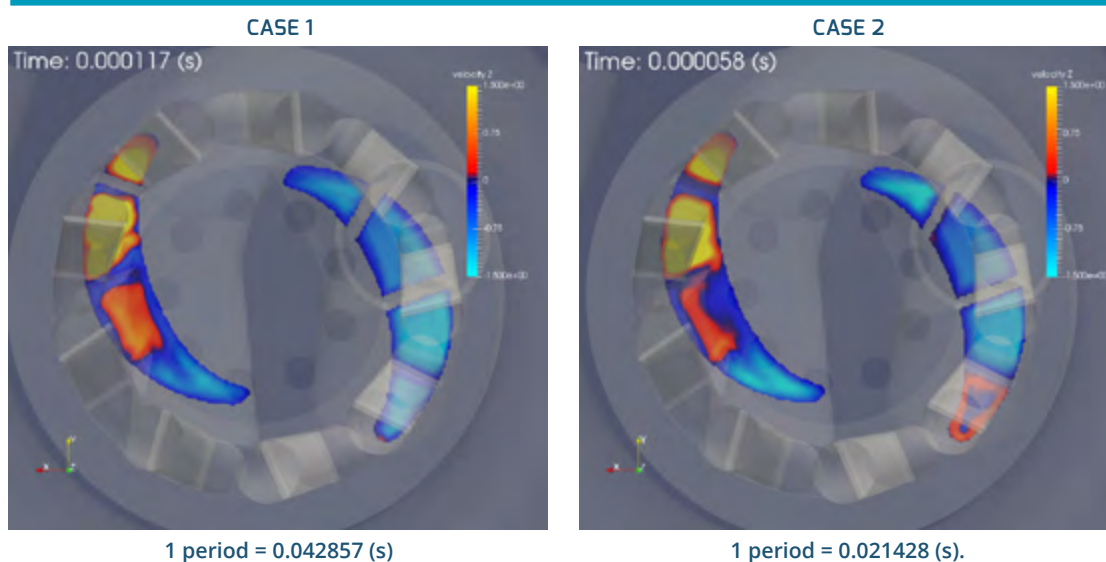


FIGURE 5: Axial velocity (m/s) - Stator cut

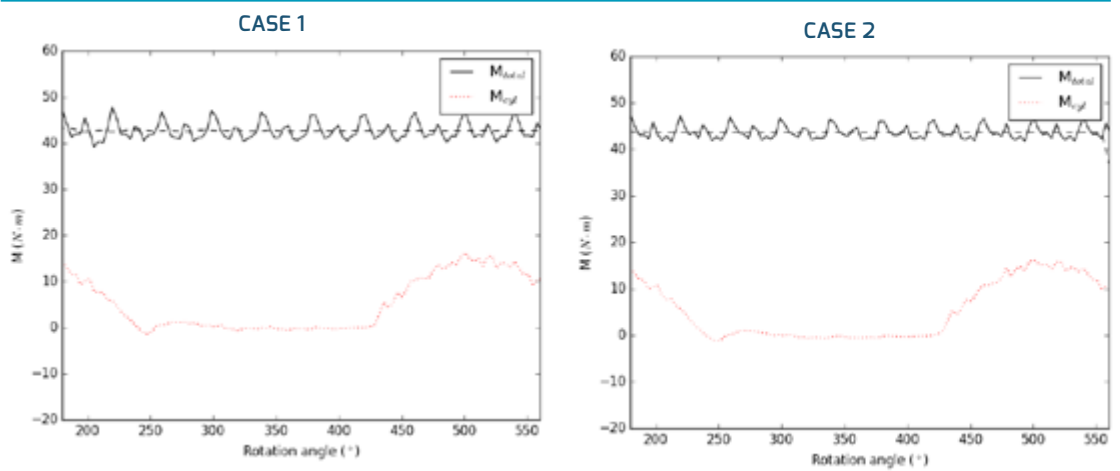


Mass flow rate contours show there is a highly complex flow overall, in the stator close to interface region. This is especially important at the cylinders, but also at the inlet and outlet passages, where an undesired backflow region is present and could be removed by improving the design. Case 1 and 2 have been selected so they attain the same mass flow rate. The property of linearity again holds, but oscillations of mass flow at the cylinders only occur in Case 2 (higher pressure and lower stroke) at the beginning of the intake stroke. The behavior for the rest of the cycle follows a smooth sinusoidal curve. The summation of the mass flow rate at all cylinders produces a fairly uniform flow from the inlet to the outlet.



3. Torque

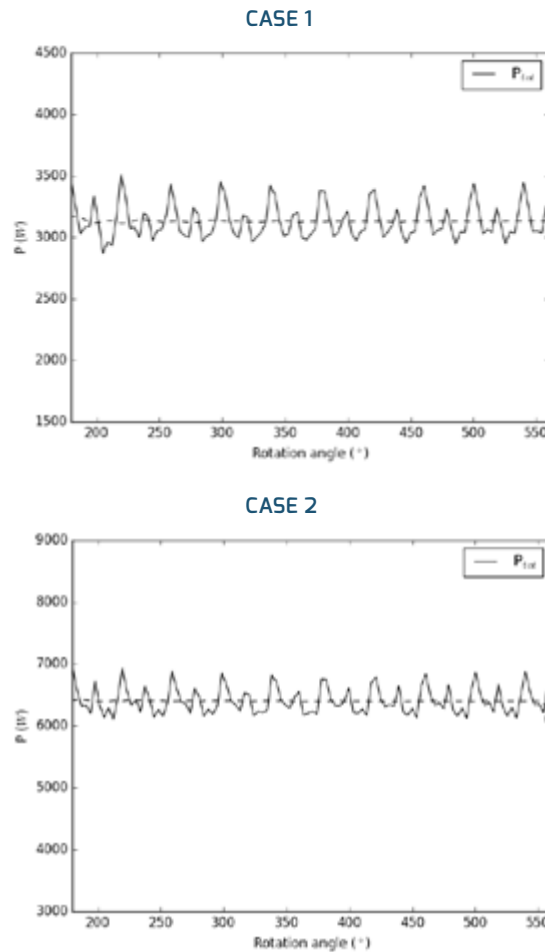
FIGURE 6 : Torque



The contribution of each piston to the torque during the intake stroke is negligible (red curve). Only during the exhaust stroke the piston exerts a substantial force against the pressurized liquid. Maximum torque is achieved when the piston is moving at its maximum speed, i.e. at the middle of the stroke. Since torque is directly related to the pressure field, the same comments apply for the comparison of both cases.

4. Power

FIGURE 7 : Power



Total hydraulic power has been obtained from the product of the torque and the rotational speed. Since Case 2 has a larger rotational speed, the power is also larger.

Conclusions

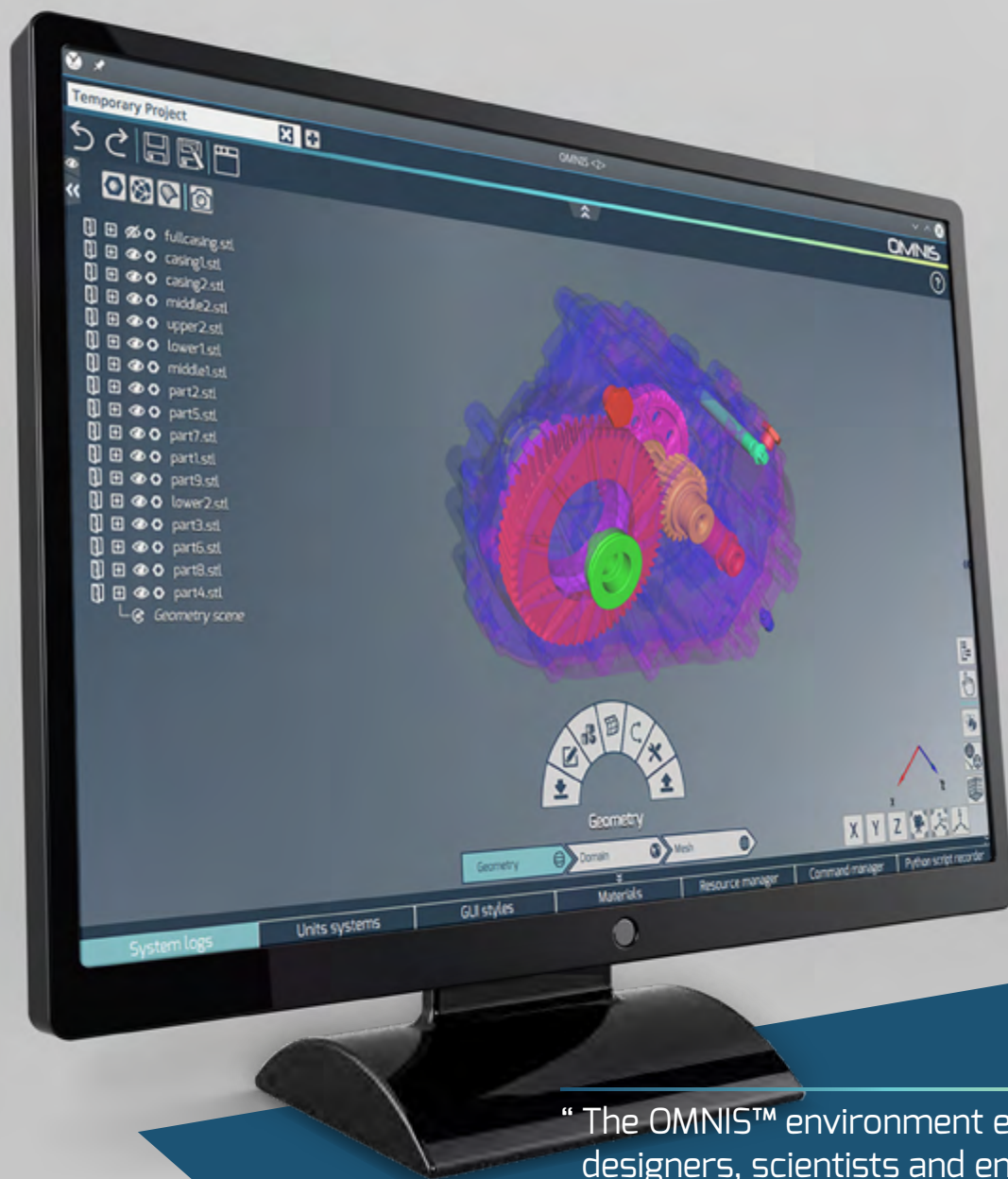
With the methodology and simulation tools proposed by NUMECA, CREMHyG has been able to compare performances at different operating conditions of the pump. The prediction of pressure and velocity in the flow through the pump given by OMNIS™/LB offers excellent quality of results while being very fast regarding time constraints. The CFD simulations presented here allowed to validate preliminary design and to better define the experimental setup (location of pressure taps).

Flow at the pump is very complex because of the sequential movement of the pistons. Rotor stator interface, without ball valves, is specific to this type of pump and produces pressure waves generated when regions of very different pressure are connected instantly. Amplitude of pressure fluctuations seems to behave linearly with the pressure difference between inlet and outlet. Consequently the cavitation risk increases in the interface region at each piston passage depending on the gradient of pressure. Backflow regions have been identified at inlet and outlet stator and its intensity depends of flow conditions. Torque and power show that flow perturbations are globally not affecting power stability. Thanks to OMNIS™/LB, pump developers can get good indications to optimize their designs based on transient analyses, therefore being able to minimize operational risks.

“ Thanks to OMNIS™/LB, pump developers can get good indications to optimize their designs based on transient analyses, therefore being able to minimize operational risks.”

This study is funded by French Government in the frame of the collaborative project Hpump.

OMNIS™: NUMECA's new generation of CAE design and optimization environment



“The OMNIS™ environment enables designers, scientists and engineers to run a full analysis and optimization chain, from preliminary to full 3D design, including robust optimization taking into account uncertainties under which the product operates.”

By **Marc Tombroff**, *General Manager,*
NUMECA International.

Industrial requirements for design based simulations cover a broad range of complex disciplines including nonlinear physics, sophisticated algorithms and numerics, cutting-edge computer science, big data, cloud access, automated workflows, intelligent optimization or man-machine interactions.

As a consequence, designers, scientists or engineers from large and medium size companies are often using a large number of CAE codes and software tools with different GUI's, data set-up, structures and formats, each of them focusing on their specific discipline, with no or poor connection between them. A more global access to the whole CAE workflow for a multidisciplinary design and optimization loop would benefit these users greatly.

An efficient industrial design system has to be able to automate a workflow composed of different CAE processes (tools and/or codes), driving them as a logical tree structure and this in batch or GUI mode, while maintaining a tight connection to CAD.

Explore, collaborate and innovate in one environment

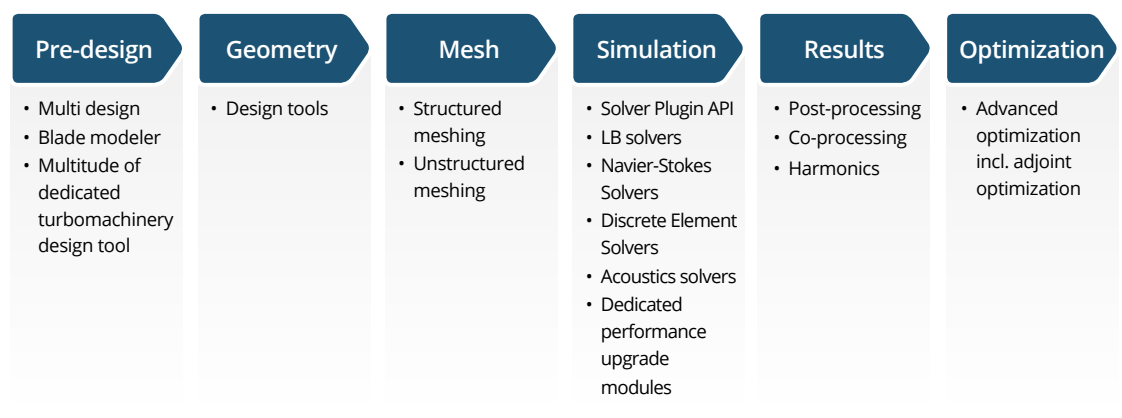
It is to address these requirements that NUMECA introduced OMNIS™. The OMNIS™ environment enables designers, scientists and engineers to run a full analysis and optimization chain, from preliminary to full 3D design, including robust optimization taking into account uncertainties under which the product operates. They can define and build their own design and optimization system and workflows, while getting access to an innovative, open and flexible software environment.

OMNIS™ can operate in 2 distinct ways: as a User Environment and/or as a Design System.

1. OMNIS™, a state-of-the-art end-to-end CAE environment

As a modern CAE software with GUI, OMNIS™ offers an impressive range of functionalities as shown in the Figure 1.

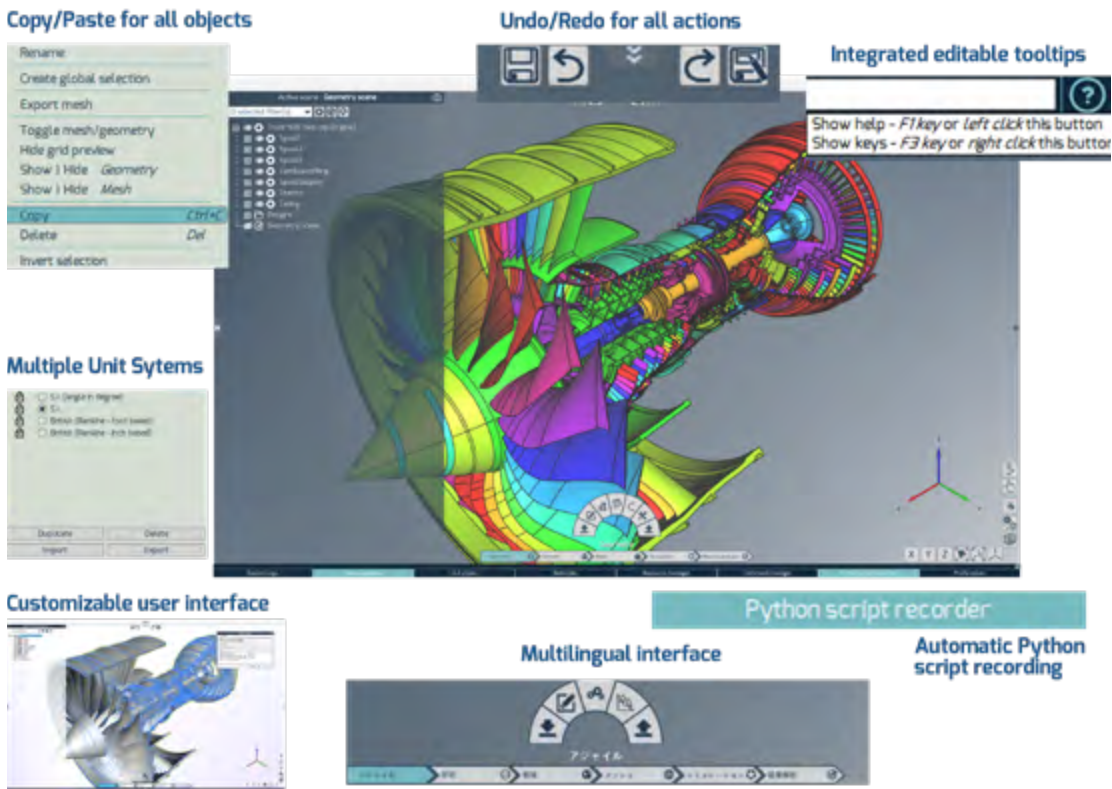
FIGURE 1 : OMNIS™'s workflow from preliminary design to optimization.



Other features include its top-level Python-based command language to operate design workflows through script or directly in OMNIS™ GUI and a unique data structure and format covering all CAE disciplines, including CAD, mesh, set-up parameters, boundary conditions and physics.

The interface provides a modern, customizable and open widget based GUI (cfr Figure 2) with Native Undo/Redo & Data Consistency for all tools as well as a Client-Server Native multi-threads and distributed technology for parallel I/O, graphics & visualization, CAD operations and multi-resolution.

FIGURE 2 : OMNIS™ environment – customizable application centric interface



2. OMNIS™ as a Design System

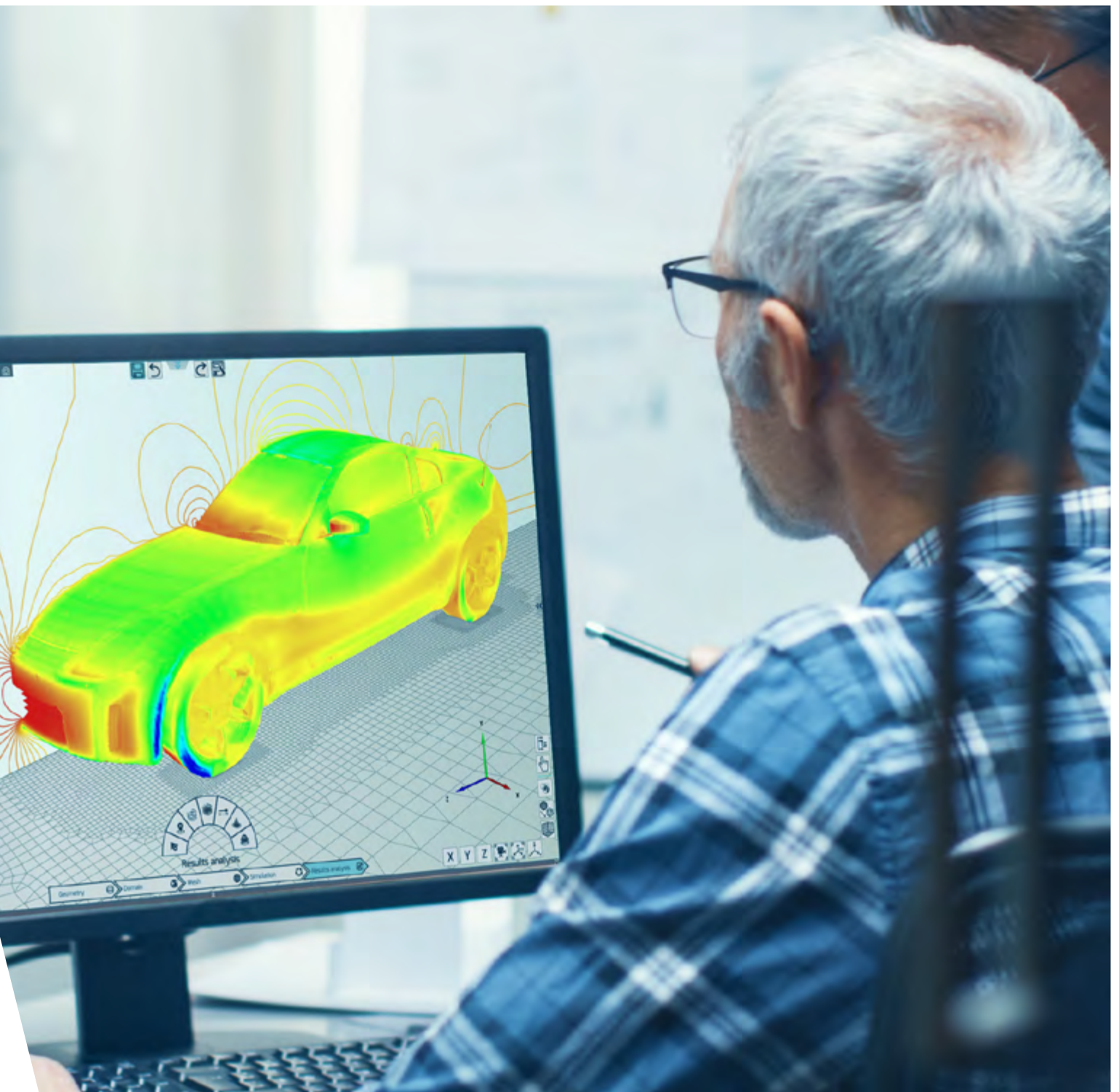
As a revolutionary approach to design methodologies, OMNIS™ has been conceived to serve as a kernel to build your own design system. OMNIS™ can drive your in-house CAE programs (CFD, FEA, Multiphysics tools and codes) through a CGNS Python HDF5 API supporting RAM based data exchange and allowing for parallel co-processing.

The Python API is currently being extended to create workflows, from simple analysis loops to complex design operations including access to our surrogate models and design optimization system, including FSI, as illustrated in Figure 3 below.

FIGURE 3 : Example of workflow to be operated in OMNIS™

```

Run CFD code with input data file_compressor_design1
If converged and if performance are > x, then
    Post-process & write report
    Run FEA code
    Extract modes
    Run flutter
    Add a domain (such as combustion chamber)
    Run full engine simulation
    Extract result and Prepare report
Otherwise move to file_compressor_design2 and go back to 1
    
```

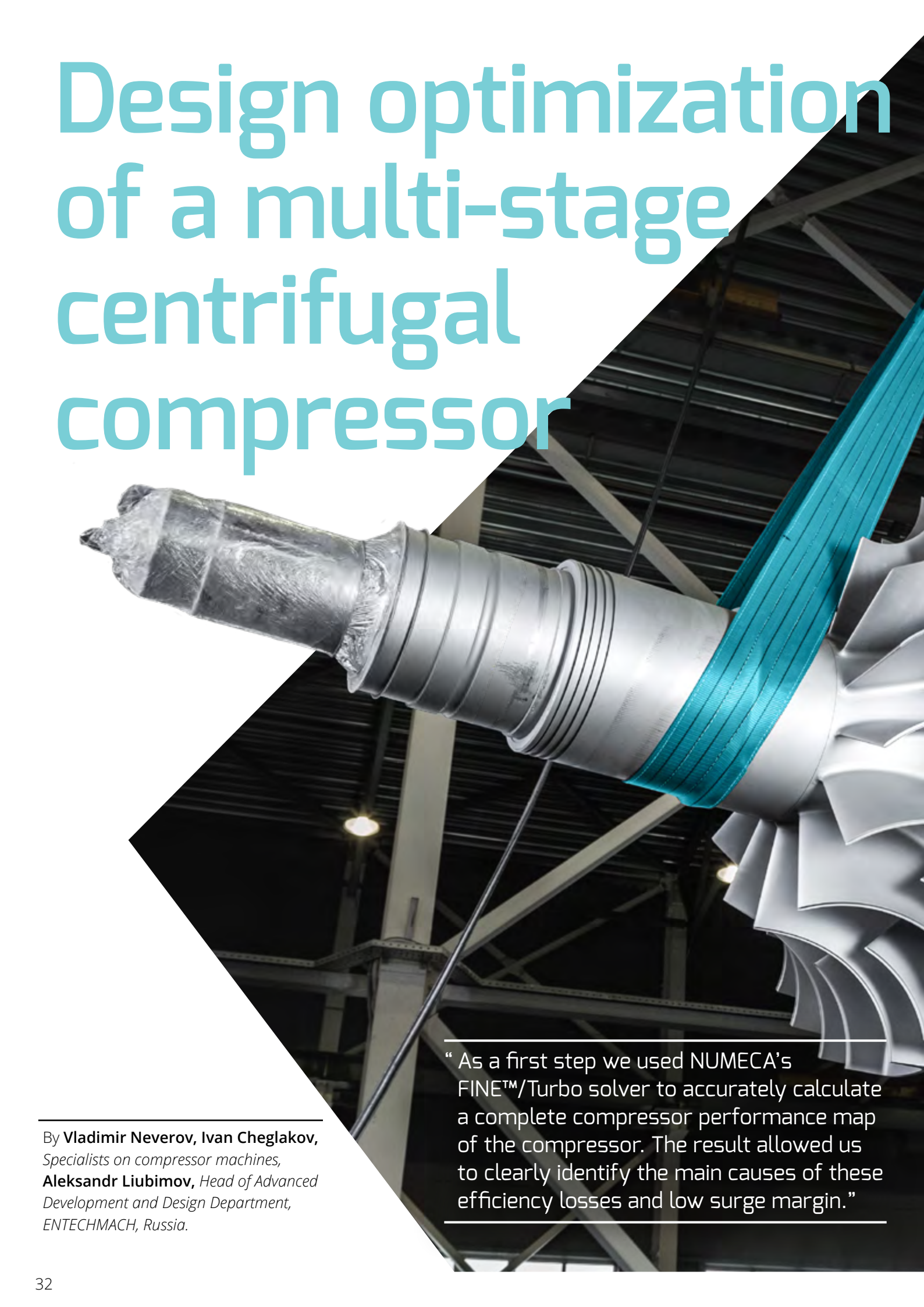


Get started

OMNIS™ as a software environment is available for download to all users. It has a shallow learning curve and is continuously being developed and extended with new functionalities and features to meet user requirements across various applications.

As a design system, OMNIS™ can be deployed on any linux/windows system, with access to its APIs and documentation to start developing your own design system.

Design optimization of a multi-stage centrifugal compressor



By **Vladimir Neverov, Ivan Cheglakov**,
Specialists on compressor machines,
Aleksandr Liubimov, *Head of Advanced
Development and Design Department,*
ENTECHMACH, Russia.

“As a first step we used NUMECA’s FINE™/Turbo solver to accurately calculate a complete compressor performance map of the compressor. The result allowed us to clearly identify the main causes of these efficiency losses and low surge margin.”



Research-and-production company «ENTECHMACH», located in Saint Petersburg, Russia, has been operating in the power engineering area for more than 25 years. Its main activities are design and production of centrifugal and axial compressors, steam turbines, multipliers, heat exchangers with air and water cooling systems.

Since 2 years ago, now the company has been using the FINE™/Turbo package for flow simulation and optimization of stationary industrial centrifugal compressors and for research engineering. One of those developments concerns the modernization project of a three-stage air centrifugal compressor in catalytic cracking technology.

Problem analysis

The existing compressor suffered a number of drawbacks: low reliability of the axi-radial impellers as their covering discs were causing large stress concentration zones, failing stators due to unsuitable material choices and a number of performance issues. The performance and discharge pressure were insufficient, the surge margin was too low and the power consumption too high.

As a first step we used NUMECA's FINE™/Turbo solver to accurately calculate a complete compressor performance map. The result allowed us to clearly identify the main causes of these efficiency losses and low surge margin. Conclusion: The modernized compressor would need a complete replacement of the rotor and stator elements in the compressor case, bearings and lubrication oil system.

Optimization

It was decided to design the new compressor with semi-opened axi-radial impellers, as they create two times less stresses compared to the closed axi-radial version with covering discs.

To make sure the newly developed impellers meet the highest possible levels of efficiency, pressure ratio and surge margin, all flow path elements were optimized with NUMECA's FINE™/Design3D solver including the impellers, the vane diffusers and the return channels for several operating conditions.

With the use of the Nonlinear Harmonic (NLH) method, the influence of the inlet chamber and 360° inlet guide vanes on first impeller parameters was investigated, as well as the influence of the outlet chamber on the last diffuser blade row. Combined vane diffusers, which merge a long vaneless part and a low blade density part, were implemented in all stages. The numerical investigations confirmed the advantages of this solution: a wide operating range and reduction of the losses in the stator elements (as with vaneless diffusers), but at the same time providing optimal flow conditions at the inlet of the return channels, which leads to an efficiency increase (as with vane diffusers).

FIGURE 1 : Second impeller streamlines

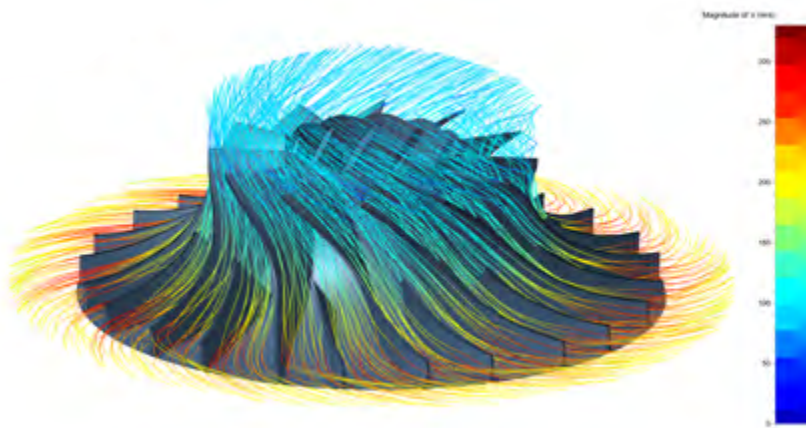


FIGURE 2 : Low density vane diffuser

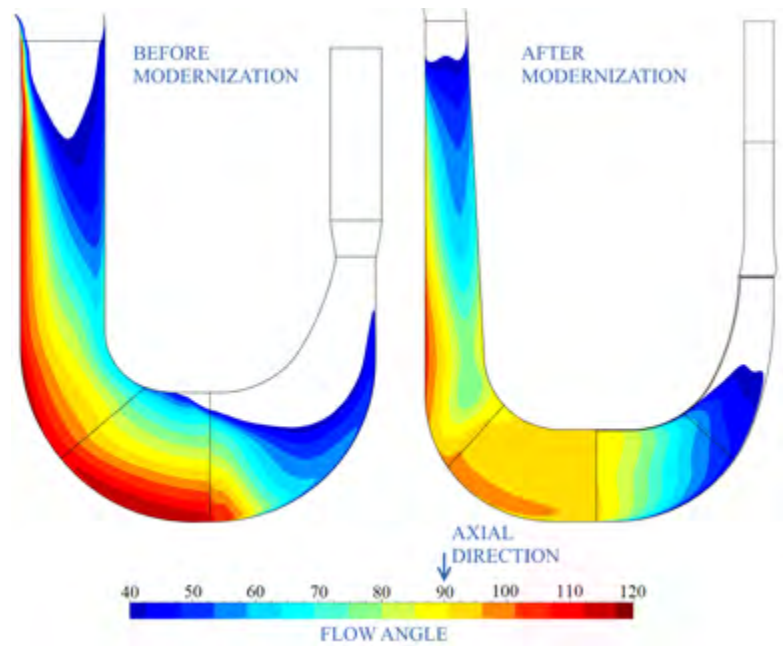


“To make sure the newly developed impellers meet the highest possible levels of efficiency, pressure ratio and surge margin, all flow path elements were optimized with NUMECA's FINE™/Design3D solver”.

The main challenge to solve for the return channel optimization was the axial flow direction at the inlet of the next impeller. Traditional return channels with 2D profiles that we analyzed, could not provide the axial flow direction on all channel spans. There were highly non-uniform flows on the hub and shroud as shown in Figure 3 on the left side.

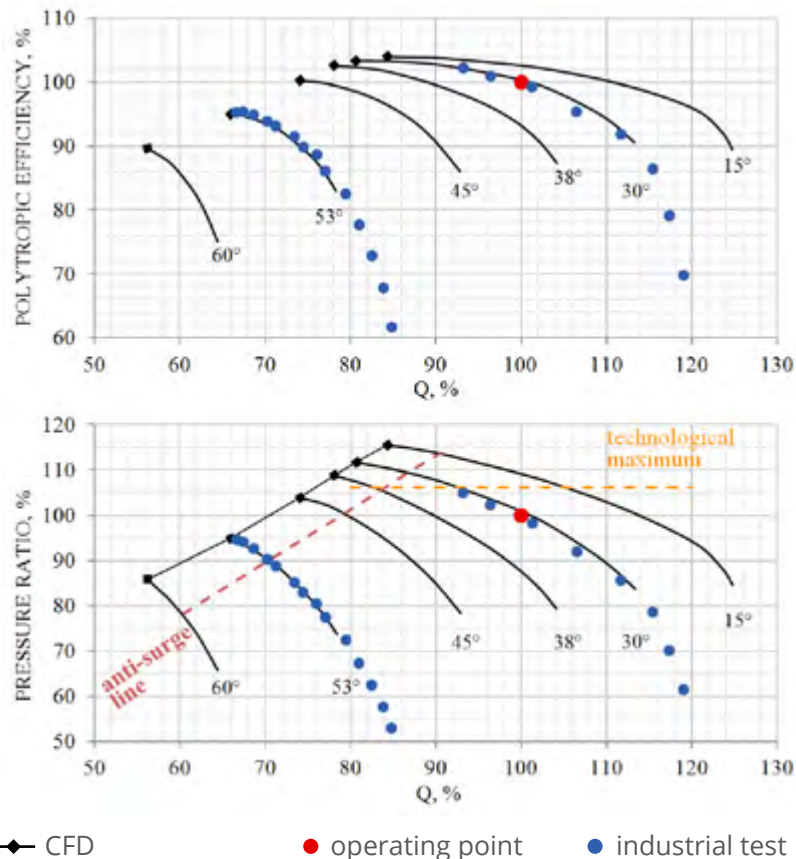
To solve this problem, we developed a non-classic return channel consisting of two parts: a 2D main profile part and a 3D outlet part. The main part was calculated in a way that would achieve the largest possible flow irregularity decrease and the 3D outlet part was designed to have an effective flow alignment on all spans. This solution suppressed the secondary flows in the return channels considerably. In Figure 3 on the right side, where 90° equals axial flow, the irregularities after the modernization can be seen. The redesigning of the return channels eventually resulted in an increase of the operating range of the second and third impellers of more than 15% thanks to the improved impeller inflow conditions.

FIGURE 3 : Flow angle



The new compressor performance map was calculated again for different operating conditions i.e. different angles of incidence of the Inlet Guide Vane (IGV) and inlet temperature. The results are shown in the Figure 4.

FIGURE 4 : Compressor performance map with different angles of incidences of IGV



Meshing

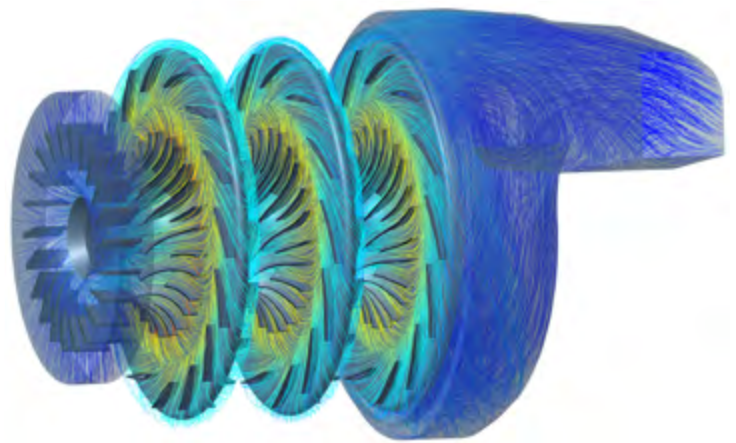
The full mesh model of the compressor was generated with IGG™ and AutoGrid5™. It included about 40 million elements and consisted of all blade rows, gaps between impellers and stator, outlet chamber and all labyrinth seal regions. The Spalart-Allmaras turbulence model for simulations was applied to verify the correspondence of mesh criterion y^+ with a recommended range. Thanks to the high quality of the mesh we could apply the CPU Booster™ for our calculations, which saved us a lot of time and computing resources.

Results

Industrial tests of the modernized compressor showed an increase of polytropic efficiency on normal mode of ~6.5% abs. and a corresponding decrease in power consumption of the same percentage. The new compressor reaches a higher pressure ratio of 4.5, compared to 4.1 before the modernization. Furthermore the surge margin related to the normal mode significantly increased from ~6% before to 50% after. Power consumption on minimal performance is 1.5 times lower (~2.5MW).

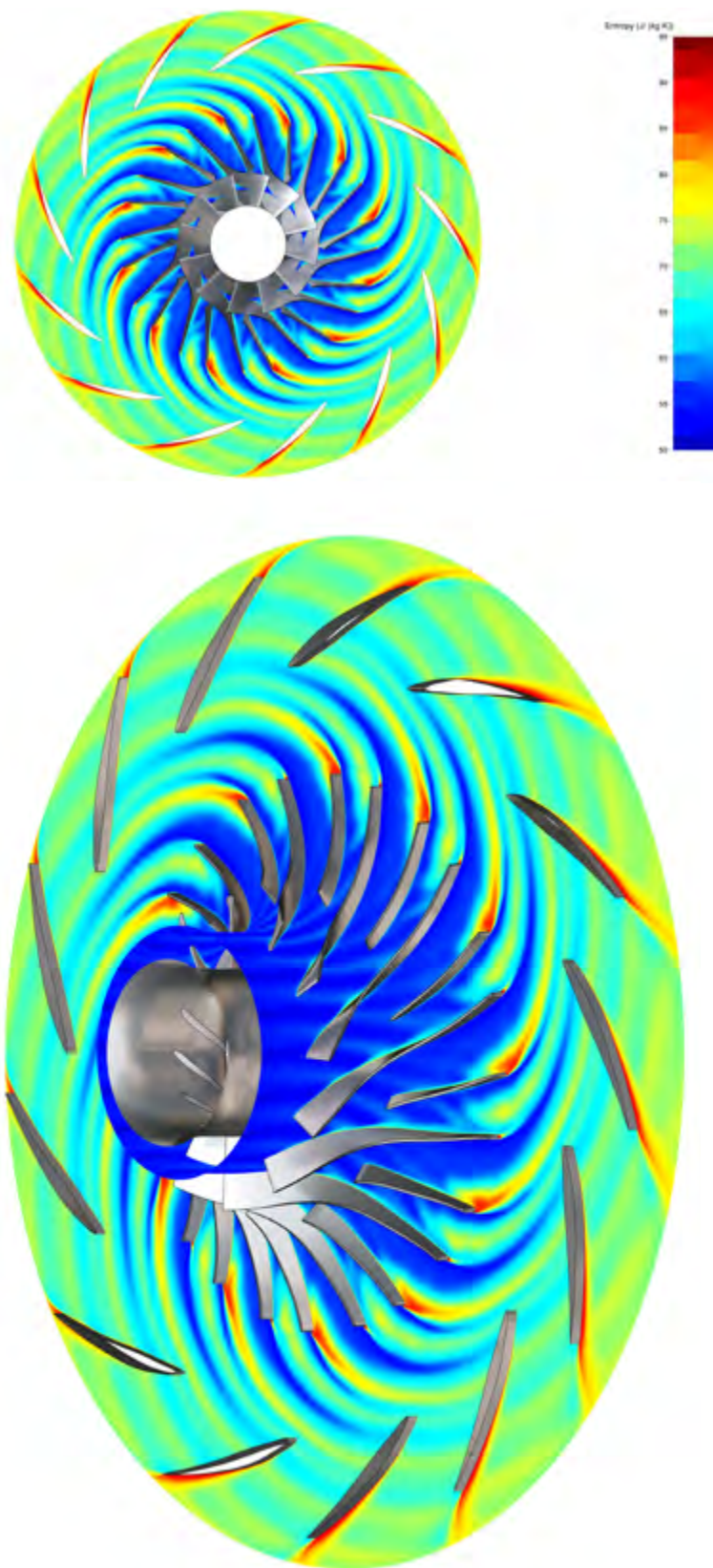
The new, modernized compressor is in operation at client site and performing well and equally as important is proving reliable.

FIGURE 5 : Full computational model of the modernized compressor



“ Thanks to the high quality of the mesh we could apply the CPU Booster™ for our calculations, which saved us a lot of time and computing resources.”

FIGURE 6 : Part of the NLH reconstruction.
Entropy passing through second impeller and diffuser



NUMECA contributes to the JAXA workshop: a NASA CRM configuration

By **Jose Botella Calatayud**, *External Consultant*
and **Benoit Leonard**, *Aero, Auto & Numerics Head of Group*,
NUMECA International.



“ The prediction of detachment in flows parallel to corners formed by intersecting walls and exposed to adverse pressure gradient remains one of the main challenges of current turbulence models widely used in industry.”

Background

The Aerodynamic Prediction Challenge (APC) is a series of workshops organized by the Japan Aerospace Exploration Agency (JAXA) with the aim of tracking the progress of CFD tools with respect to challenges faced in aeronautical applications. NUMECA took part in the last APC edition as contributor to Task 1, with NASA Common Research Model (CRM) aerodynamic prediction at cruise state and high angle of attack (presence of tail wings, reflected deformation measurement data).

Task description

The model under investigation is a 80% scaled copy of CRM at high speed (cruise state). CRM was developed by Boeing and NASA for the purpose of validating CFD drag predictions, with focus on the aerodynamic design of the wing. The selected configuration includes horizontal tail plane (HTP) at zero setting angle, which is the configuration used for the NASA Drag Prediction Workshop 4 (DPW4).

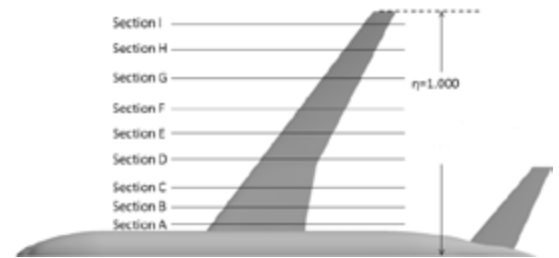
A wind tunnel test (WTT) of the 80% scaled copy of the CRM was performed in the 2m × 2m transonic wind tunnel of JAXA and is therefore used as benchmark to assess numerical results provided by participants. Flow conditions correspond to Mach number $M=0.847$ and Reynolds number (based on wing mean aerodynamic chord) $Re=2.26 \text{ E}+06$.

Emphasis in the analysis of results is given to high angle of attack, particularly in the wing-fuselage junction. The prediction of separation in the wing-fuselage juncture, exposed to adverse pressure gradient remains one of the main challenges of current turbulence models widely used in industry.

Deliverables requested by the organizing committee included Aerodynamic coefficients (C_d , C_l , C_m) with decomposition into pressure

and friction, breakdown by components (wing, fuselage, HTP), and pressure coefficient distribution along nine wing sections distributed spanwise.

FIGURE 1 : 80% scaled copy of the CRM was performed in the 2m × 2m transonic wind tunnel of JAXA. Spanwise wing sections distribution.



CFD simulations

Two sets of meshes were provided by JAXA to all participants, a structured mesh and a hybrid tetrahedral dominant mesh. Cell count was 9.15 and 29.98 million respectively. The difference in cell count is due to additional refinement for the hybrid grid at the leading and trailing edges of lifting surfaces, notably in spanwise direction (cfr Figures 2 and 3).

Aeroelastic effects are taken into account using one mesh for each of the incidence angle of the range under investigation (-1.79 deg. - 5.72 deg.), which accounted for wing deformation data measured during WTT. The near wall mesh is very fine, with non-dimensional wall distance of first cell in the viscous sublayer ($y^+ < 1$).

FIGURE 2 : Overview of structured and hybrid grids of CRM model.

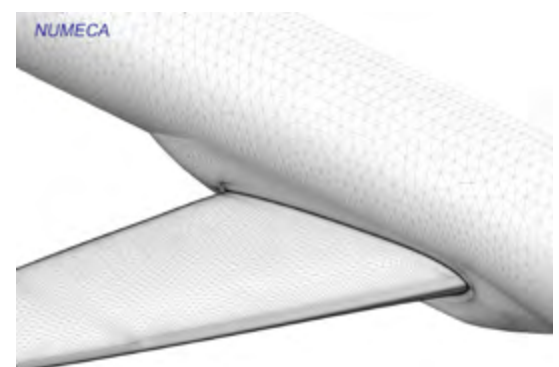
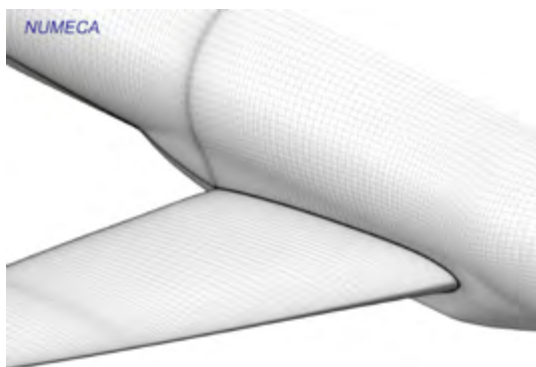
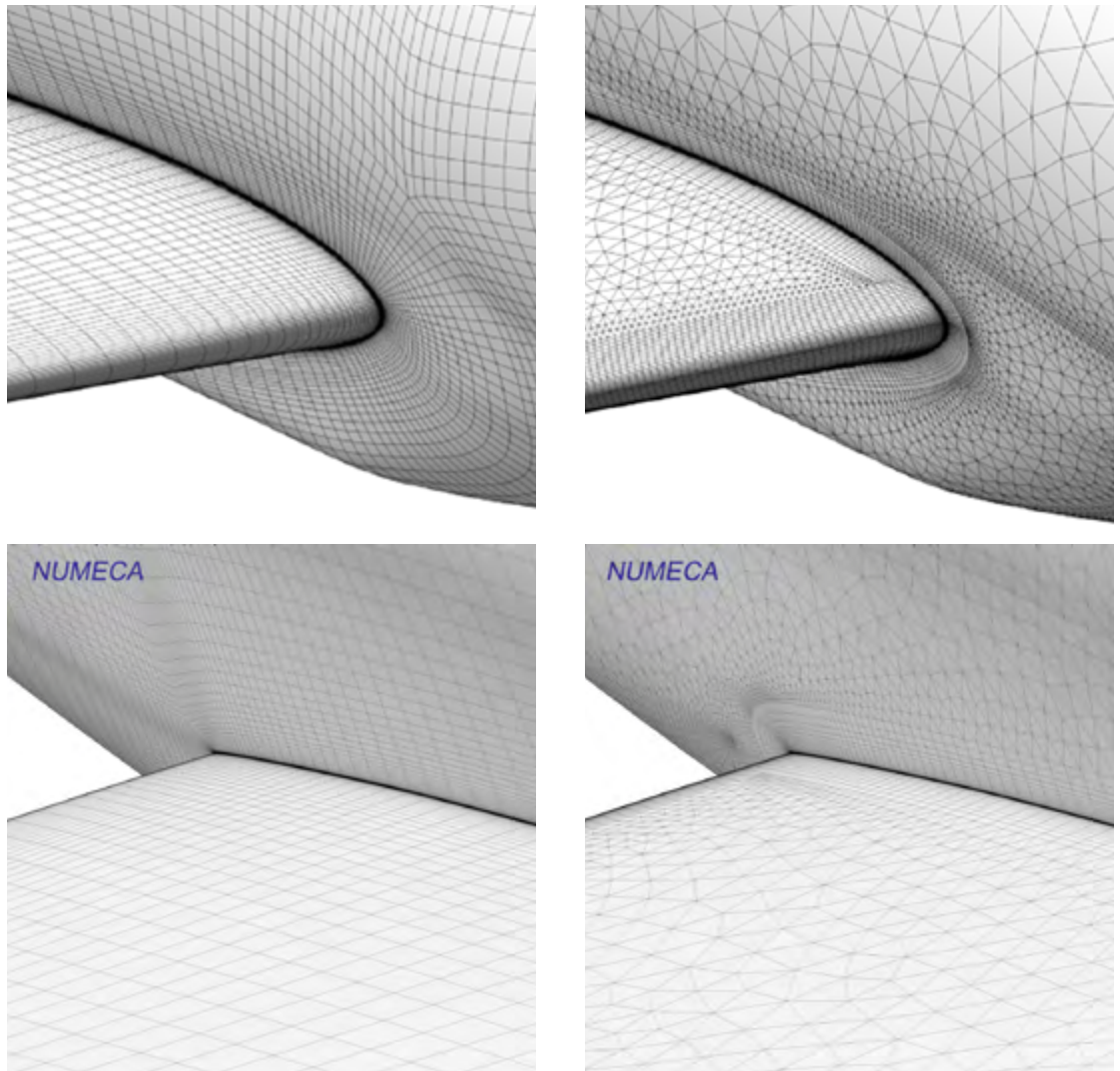


FIGURE 3 : Details of structured and hybrid grids of CRM model.



NUMECA FINE™/Open 6.2 CFD solver (density based, finite volume discretization, cell centred) was used to solve the Reynolds averaged Navier-Stokes (RANS) equations with full multigrid approach and different turbulent formulations:

Several turbulence models were investigated by NUMECA, comparing their adequacy at the higher incidences, dominated by wing-fuselage corner separation. The models considered cover the Linear eddy viscosity models (LEVM) of Spalart-Allmaras SA-fv3, Menter SST-2003 and the Yang-Shih K-Epsilon KE-YS-1993. As

well as two Explicit Algebraic Reynolds Stress Models (EARSM) with a non-linear constitutive relationship between Reynolds stresses and mean strain rate, namely the SBSL-EARSM and a new model, SSC-EARSM, developed by NUMECA with the aim of better predicting separated flows.

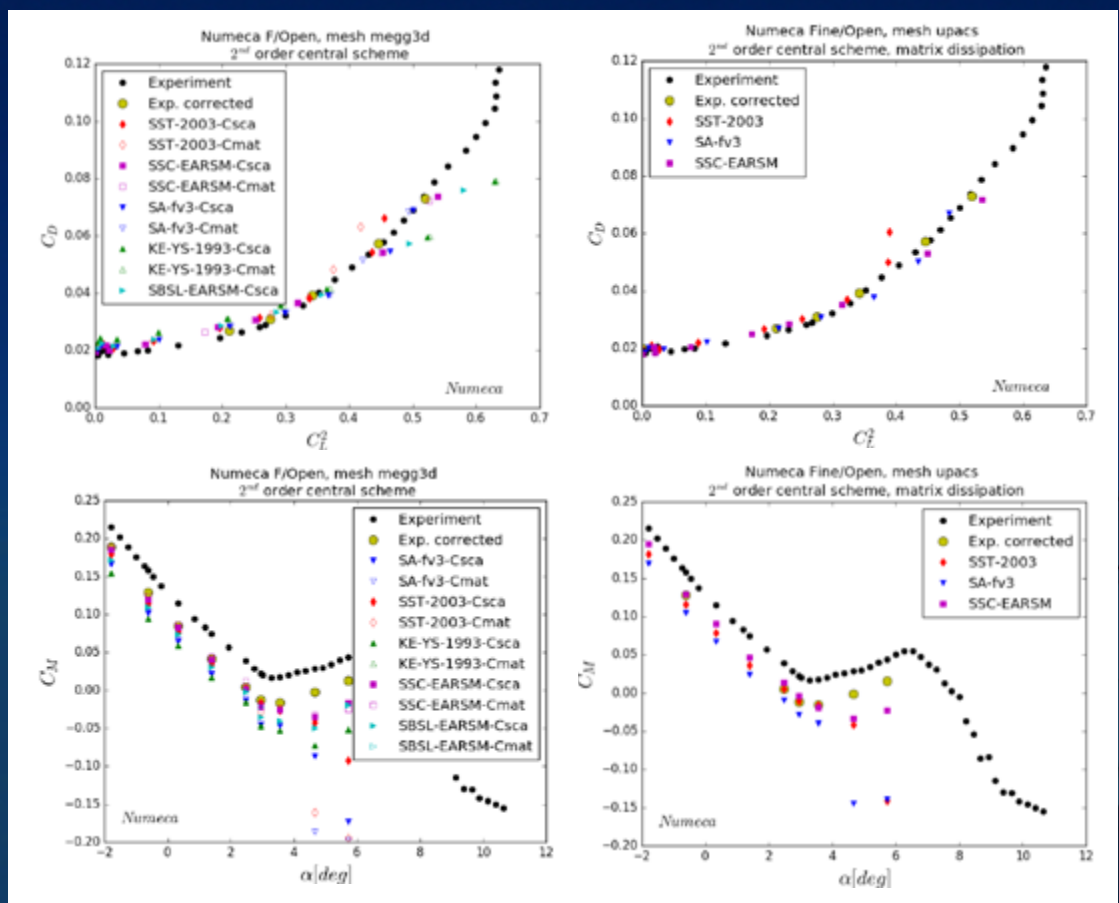
Moreover, the study is also evaluating the impact of numerical artificial dissipation and its interaction with the turbulence models, comparing scalar (C_{sc}) and matrix dissipation (C_{mat}) in the central scheme.

Results

Figure 4 summarizes the results with different turbulence models and dissipation options. A first observation is the high sensitivity of the SST model to the numerical dissipation, which is a new result, hardly mentioned in the literature.

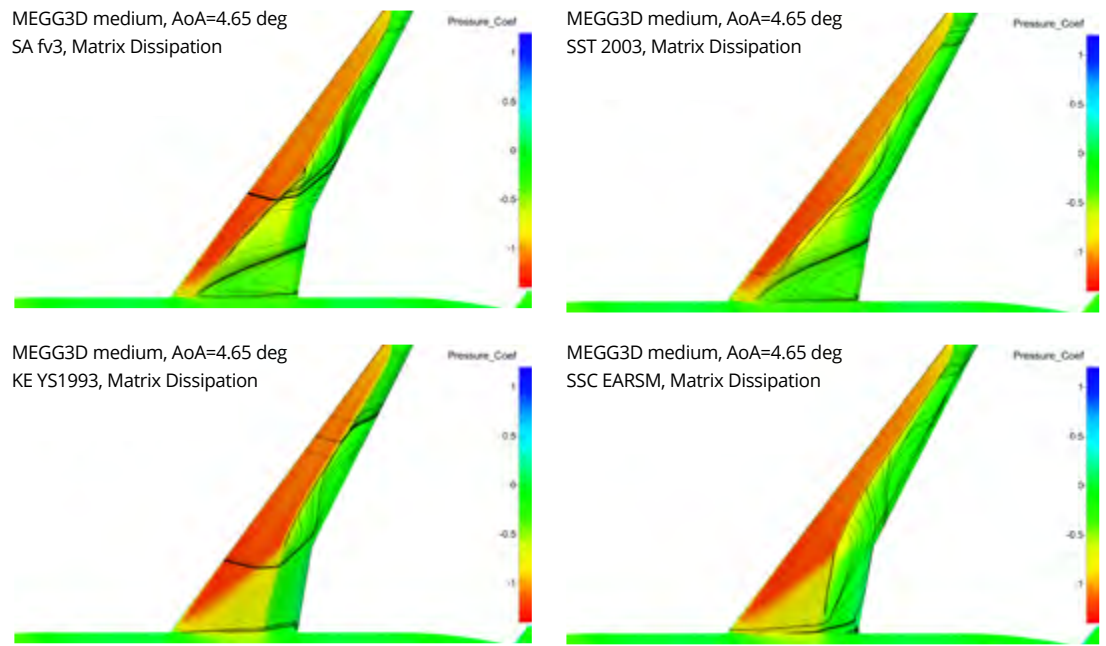
At higher incidences, the turbulence models and the dissipation models have a large impact on the solution, which is especially noticeable in the pitching moment and its slope (which drives longitudinal stability). Analysis of pressure distribution over wing suction side explain those differences, as seen from Figures 5 and 6.

FIGURE 4 : Polar (top) and pitching moment (bottom) results for the structured (right) and hybrid (left) grids.



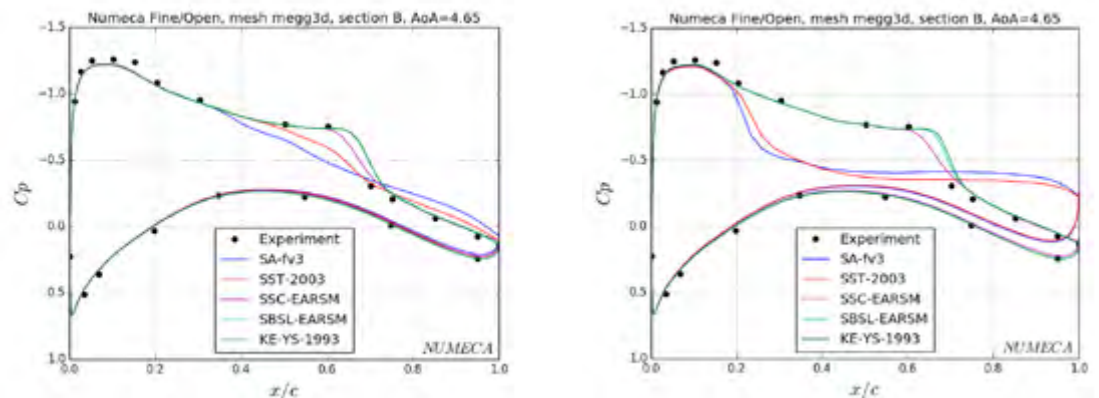
Excessive corner separation is predicted by SA-fv3 and SST-2003 models at high incidence, which is not in line with experimental data and leads to different flow patterns for the whole span and lower pitching moment. This corner separation is not observed with KE-YS-1993, which predicts a shock wave location significantly downstream, overestimating the lift. On the other hand, the SBSL-EARSM and SSC-EARSM models improve the predicted inboard flow and the location of shocks in this region.

FIGURE 5 : Pressure distribution over wing suction side at angle of attack 4.65 deg. for several turbulence models with matrix artificial dissipation.



Pressure coefficient cuts show that the SSC-EARSM model, developed by NUMECA specifically for separated flows prediction, provides the best agreement with experimental data, independently of the mesh topology and numerical dissipation scheme.

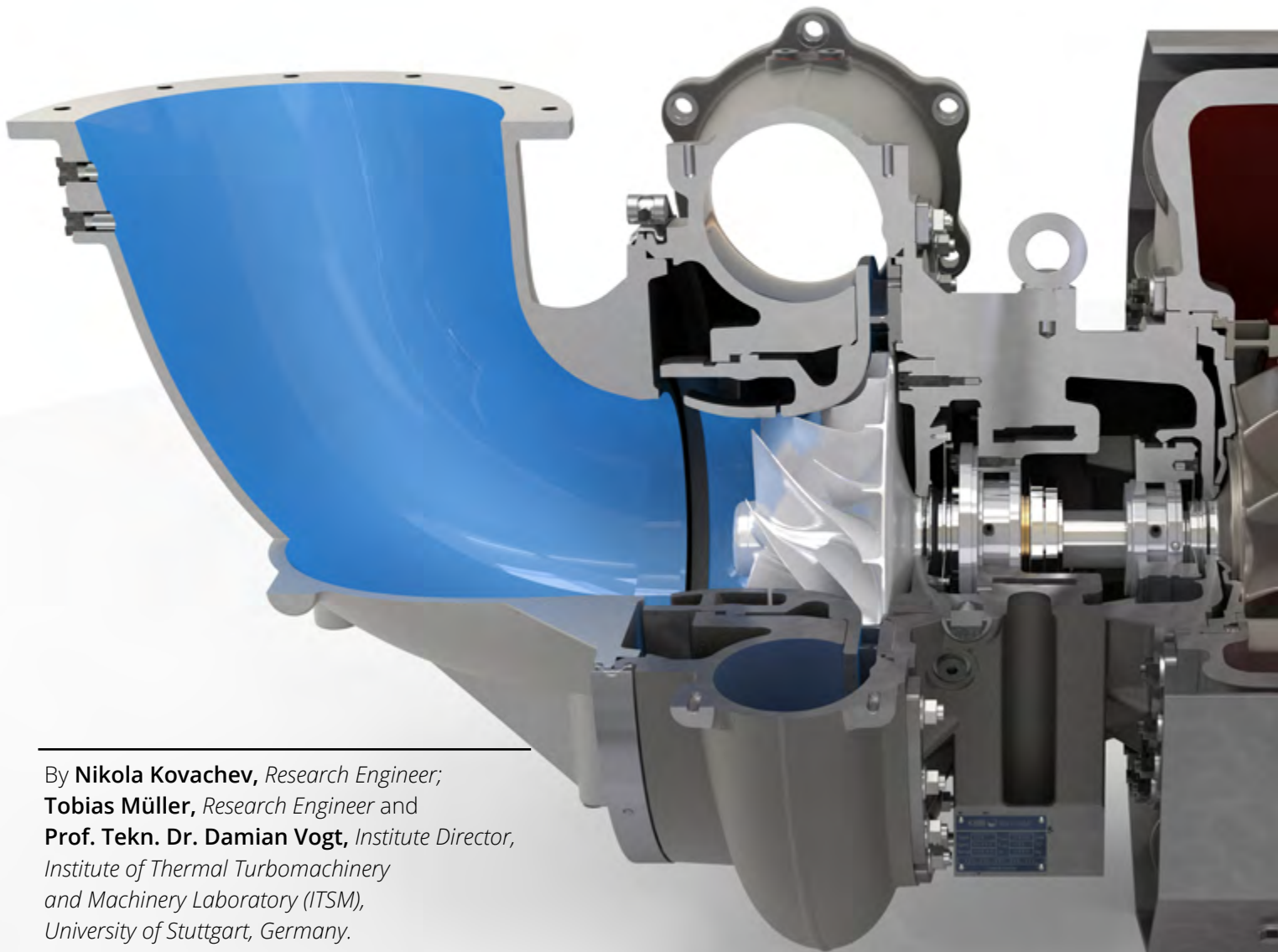
FIGURE 6 : Pressure distribution over wing section at 20.1% of span at angle of attack 4.65 deg. for several turbulence models with scalar dissipation (left) and matrix dissipation (right) computed on hybrid grid.



Source: Jose Botella Calatayud, Benoit Leonard, Lionel Temmerman, and Charles Hirsch. "Sensitivity to Turbulence Models and Numerical Dissipation of the CRM Drag Prediction", 2018 Applied Aerodynamics Conference, AIAA AVIATION Forum, (AIAA 2018-3332) <https://doi.org/10.2514/6.2018-3332>.

“ NUMECA SSC-EARSM results are encouraging, with significantly improved results with respect to traditional LEVM and with affordable computational cost.”

Accurate and reliable prediction of the unsteady flow in a radial turbine



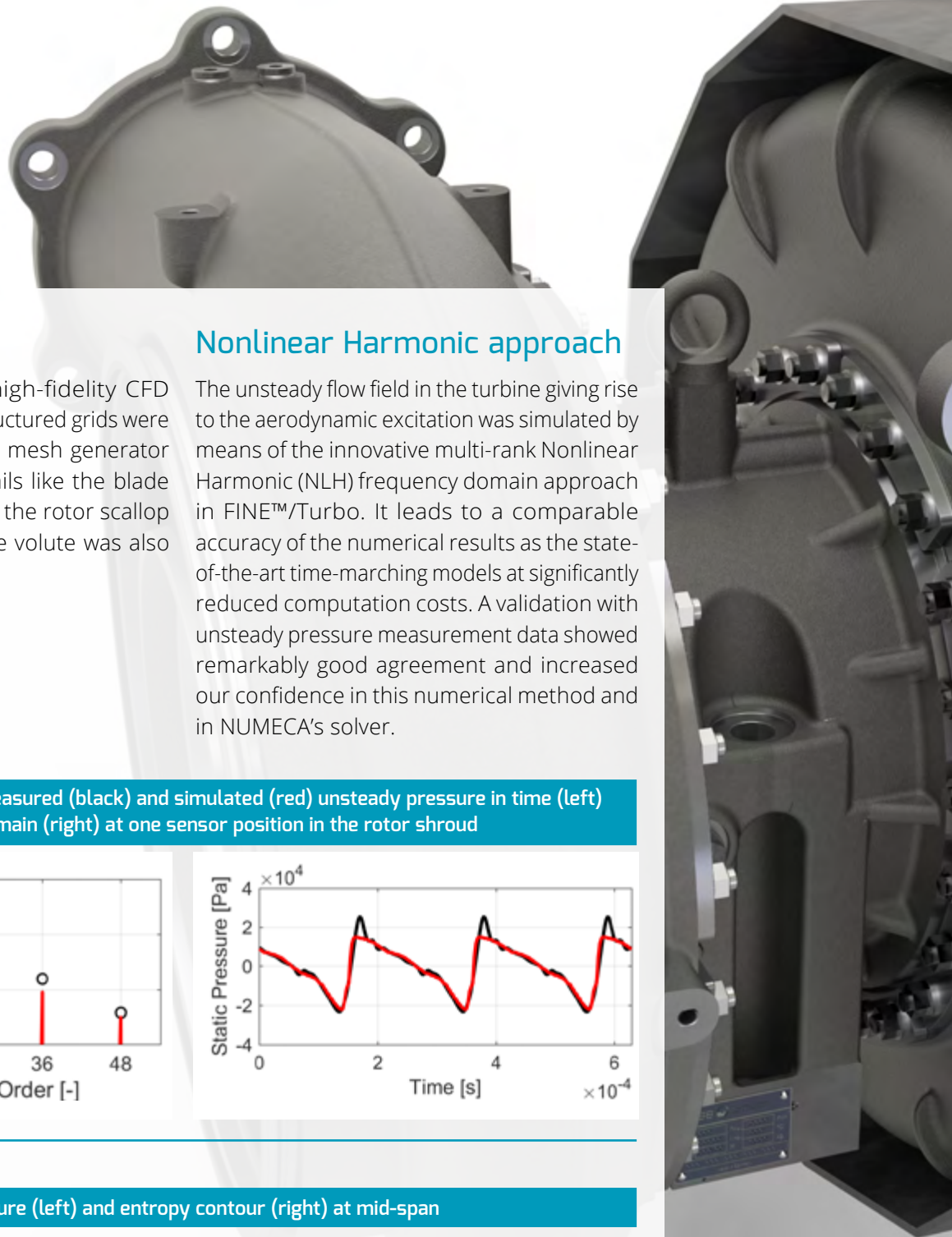
By **Nikola Kovachev**, *Research Engineer*;
Tobias Müller, *Research Engineer* and
Prof. Tekn. Dr. Damian Vogt, *Institute Director*,
*Institute of Thermal Turbomachinery
and Machinery Laboratory (ITSM),
University of Stuttgart, Germany.*

The Institute of Thermal Turbomachinery and Machinery Laboratory (ITSM) of the University of Stuttgart, based in Germany, focuses its research on gas turbines, steam turbines and turbochargers. As part of the FVV-funded project "Blade Forces", NUMECA software tools were utilized. The goal was to develop a workflow for accurate, reliable and affordable prediction of forced response vibrations in radial turbines, taking into account mistuning effects. A thorough validation of this workflow was conducted experimentally and numerically.

FIGURE 1 : CFD Model of the investigated radial turbine



“ A validation with unsteady pressure measurement data showed remarkably good agreement and increased our confidence in this numerical method and in NUMECA’s solver.”



Meshing

On the numerical side, high-fidelity CFD models comprising block-structured grids were created with the automatic mesh generator AutoGrid5™, including details like the blade tip gap and fillets as well as the rotor scallop and backspace. The turbine volute was also included in the model.

Nonlinear Harmonic approach

The unsteady flow field in the turbine giving rise to the aerodynamic excitation was simulated by means of the innovative multi-rank Nonlinear Harmonic (NLH) frequency domain approach in FINE™/Turbo. It leads to a comparable accuracy of the numerical results as the state-of-the-art time-marching models at significantly reduced computation costs. A validation with unsteady pressure measurement data showed remarkably good agreement and increased our confidence in this numerical method and in NUMECA's solver.

FIGURE 2 : Comparison of measured (black) and simulated (red) unsteady pressure in time (left) and frequency domain (right) at one sensor position in the rotor shroud

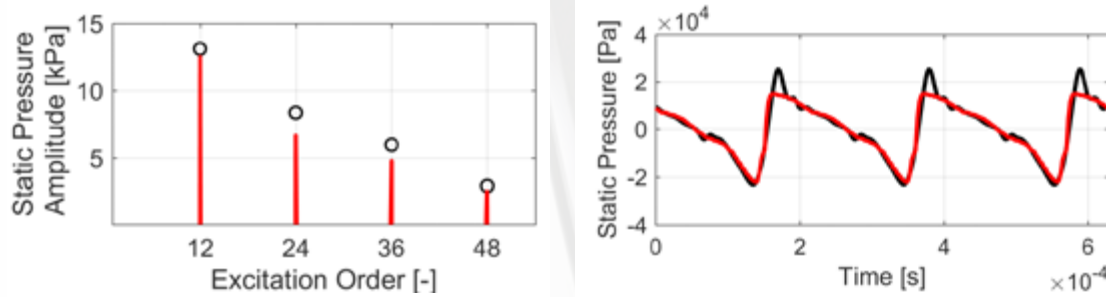
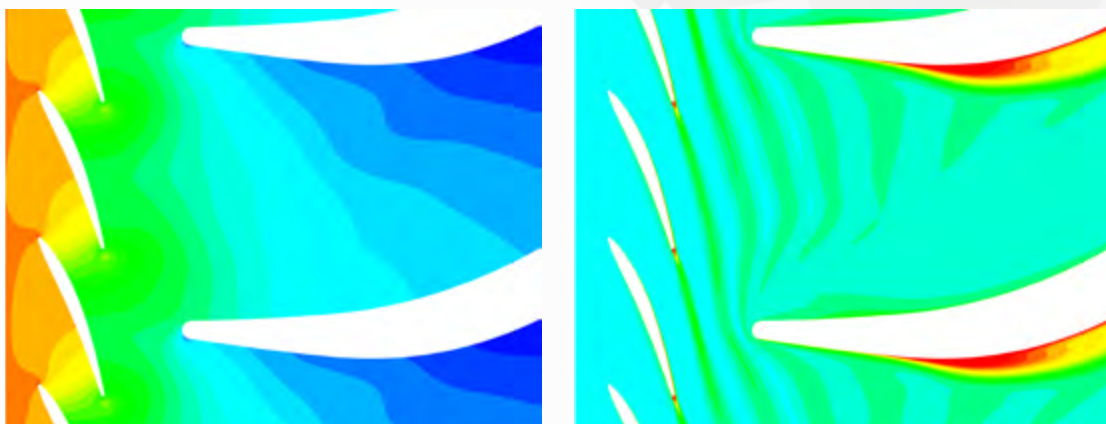
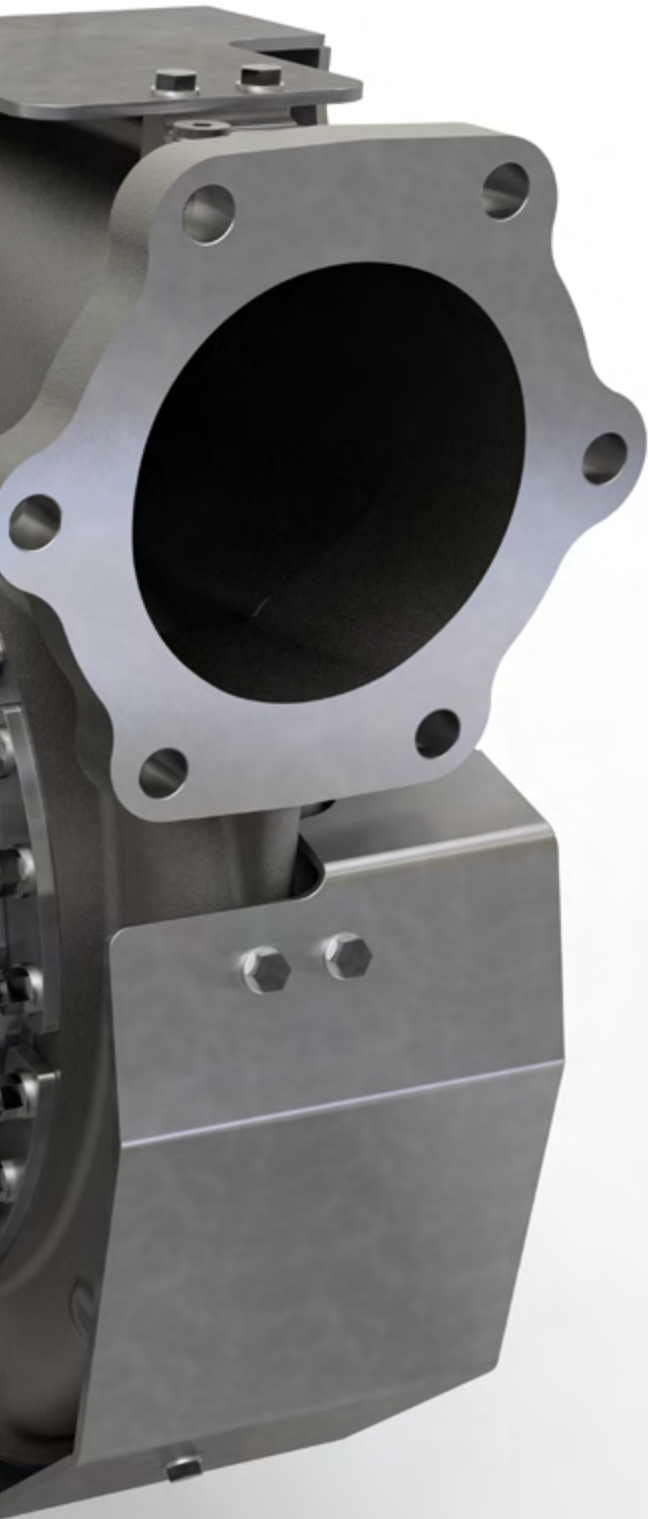


FIGURE 3 : Mean static pressure (left) and entropy contour (right) at mid-span





Aerodynamic damping

The aerodynamic damping in the turbine was also predicted by means of the NLH method. For this purpose, the mode shapes of the investigated resonance crossings as obtained from a prior modal analysis were applied as an elastic blade vibration with defined vibration amplitude. By utilizing the NLH method, aerodynamic damping was computed with high accuracy and low computation time.

Given the excellent performance of NUMECA's software tools, we look forward to employ them in other projects and to continue our cooperation with NUMECA as an academic partner.

FIGURE 4 : Distribution of the instantaneous blade surface disturbance pressure giving rise to aerodynamic excitation.

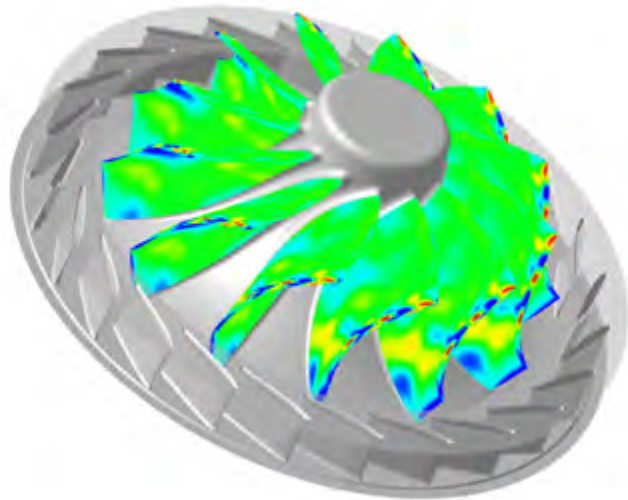
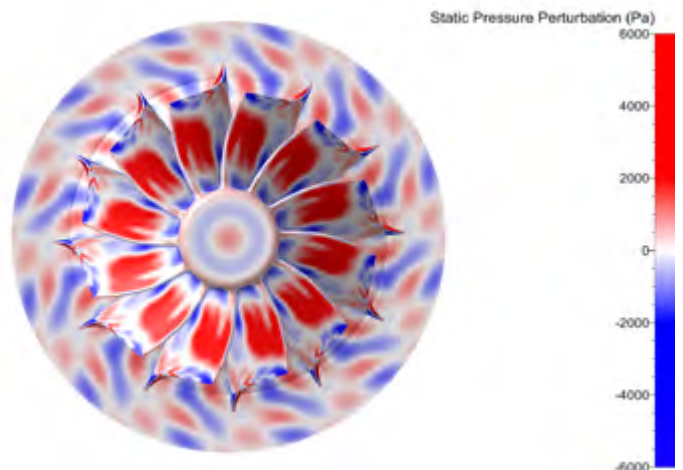


FIGURE 5 : Distribution of the instantaneous blade surface disturbance pressure giving rise to aerodynamic damping.



NUMECA International

USER MEETING 2019

BRUSSELS, NOVEMBER 12-14, 2019

Registration and call for papers:

www.numeca.com/usermeeting2019



NUMECA International

Ch. de la Hulpe 189 Terhulpe Steenweg
1170 Brussels - Belgium
+32 (0)2 647 83 11

www.numeca.com
Contact us: info@numeca.be

Advanced developments for better products